The Fano Incidence Graph, alias Heawood Graph and 6-Cage

Edward Anderson*

Abstract

These are Projective Geometry, graph-colouring and extremal-graph names respectively for the same, consequently venerable, graph. Standard bipartite, Hamiltonian, minimum-crossing, and torus presentations are exhibited and discussed. Alongside new bipartite and Flat Geometry presentations arising from basic Topological, Geometrical and Graph Drawing and Visualization considerations. These ideas transcend to other incidence graphs and bipartite graphs more generally. Some of this graph's many heirs are also outlined.

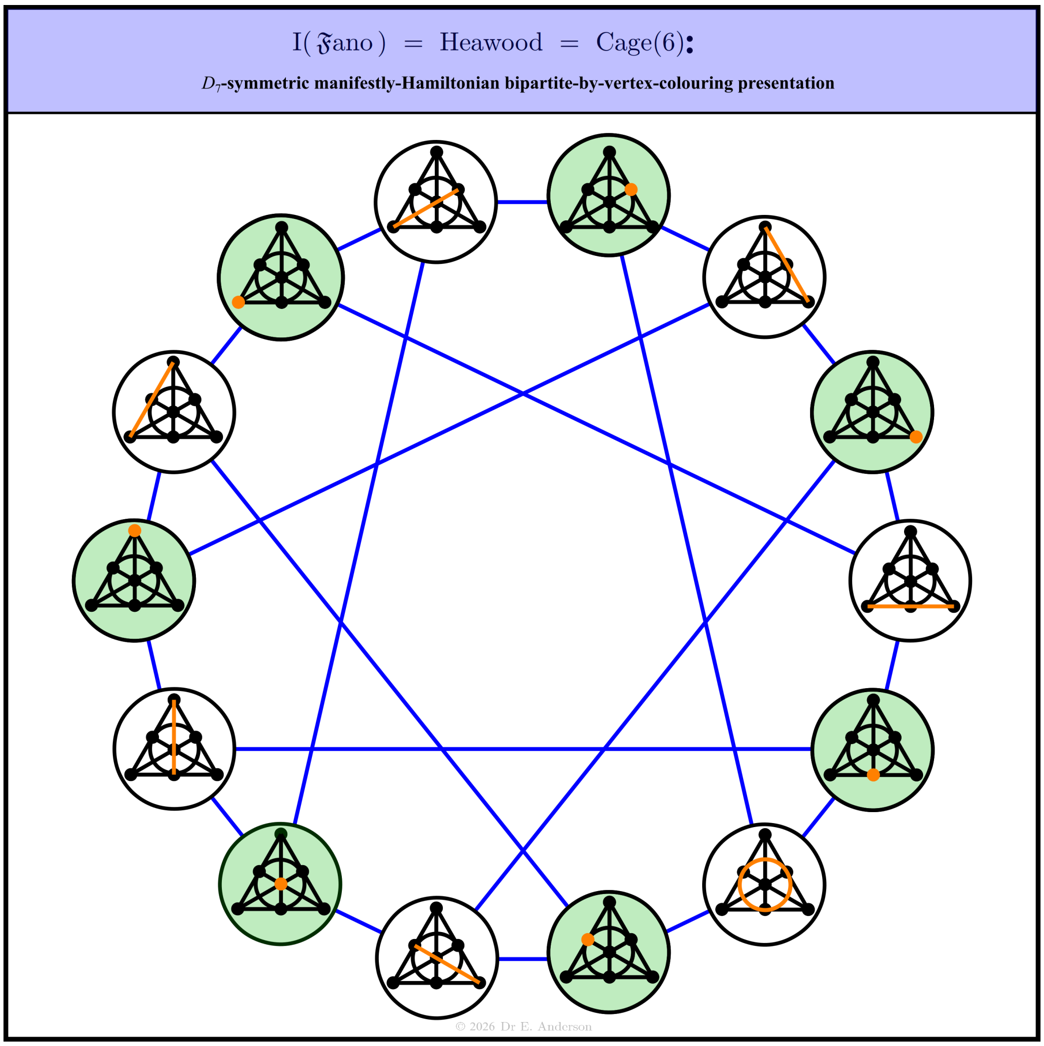

Figure 1:

The bulk of this Article is ⟨3⟩: accessible to third-year undergraduates.

Date stamps: v1 17-04-2026, v2 07-05-2026.

Cite as: E. Anderson, "The Fano Incidence Graph, alias Heawood Graph and 6-Cage" Online Encyclopaedia of Applied Graph and Order Theory institute-theory-stem.org/oeagot-fano-incidence-graph/ (2026) .

* Dr.E.Anderson.Maths.Physics *at* protonmail.com . Institute for the Theory of STEM

1 Introducing the Fano configuration and its incidence graph

1.1 Motivation

Remark 1 *Projective Geometry* ⟨2-3⟩ [90, 69, 71, 64, 68, 72] is Geometry pared down to the study of *incidence*. Suppose that one considers objects no higher than Projective planes [89, 50], as is suitable for 2-d and 2-d-inspired Geometry. Then incidence is a binary relation on points-and-lines. Comprising points lying on lines and lines passing through points.

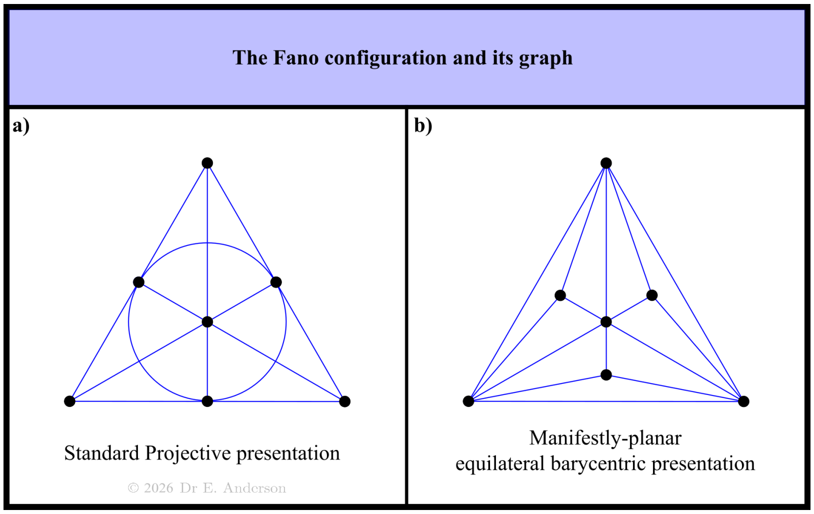

Figure 2:

Remark 2 We previously outlined [50] how Fano's configuration is the smallest projective plane. Identified the corresponding Fano (configuration) graph Fano (Fig 2). And proceeded to study some of its elementary properties and nice drawing and visualization [42] presentations. We now consider instead the corresponding incidence graph, following Coxeter's recommendation [7] grounded in faithfulness.

Definition 1 Suppose that we are given a Projective (or more generally Incidence) Geometry [78, 81, 92]) configuration. Then the corresponding *incidence graph* alias *Levi graph* [4, 7, 89, 36, 83] represents each point and line in the configuration by the vertices of a graph. With edges between point-vertices and line-vertices wherever the point and line in question are incident.

1.2 Incipient manifestly-bipartite presentation

Remark 1 Incidence graphs for Projective point-and-line configurations are always bipartite. The configuration's points form one part, and the configuration's edges the other. When Projective duality is present, it dictates that these 2 parts are to be of the same size: a 'homobipartite' graph.

Remark 2 Every Projective point-and-line configuration's incidence graph admits a natural incipient bipartite presentation. In the Fano case, we provide a such in Fig 3.

1.3 Some of this Encyclopedia's notation

Notational Remark 1 Our own strategy for depicting small to middle-sized graphs (say 1 to 50 vertices) whose vertices themselves represent Combinatorial objects is as follows. We use large figures in which the vertices are labelled by pictorial presentations of the Combinatorial objects themselves. For some balance of optimal and well-known presentations of these Combinatorial objects.

Notational Remark 2 Using highlighted subsets of the Fano graph rather than introducing meaningless labels for vertices is an example of truer-denotation. In studying the Combinatorics of a

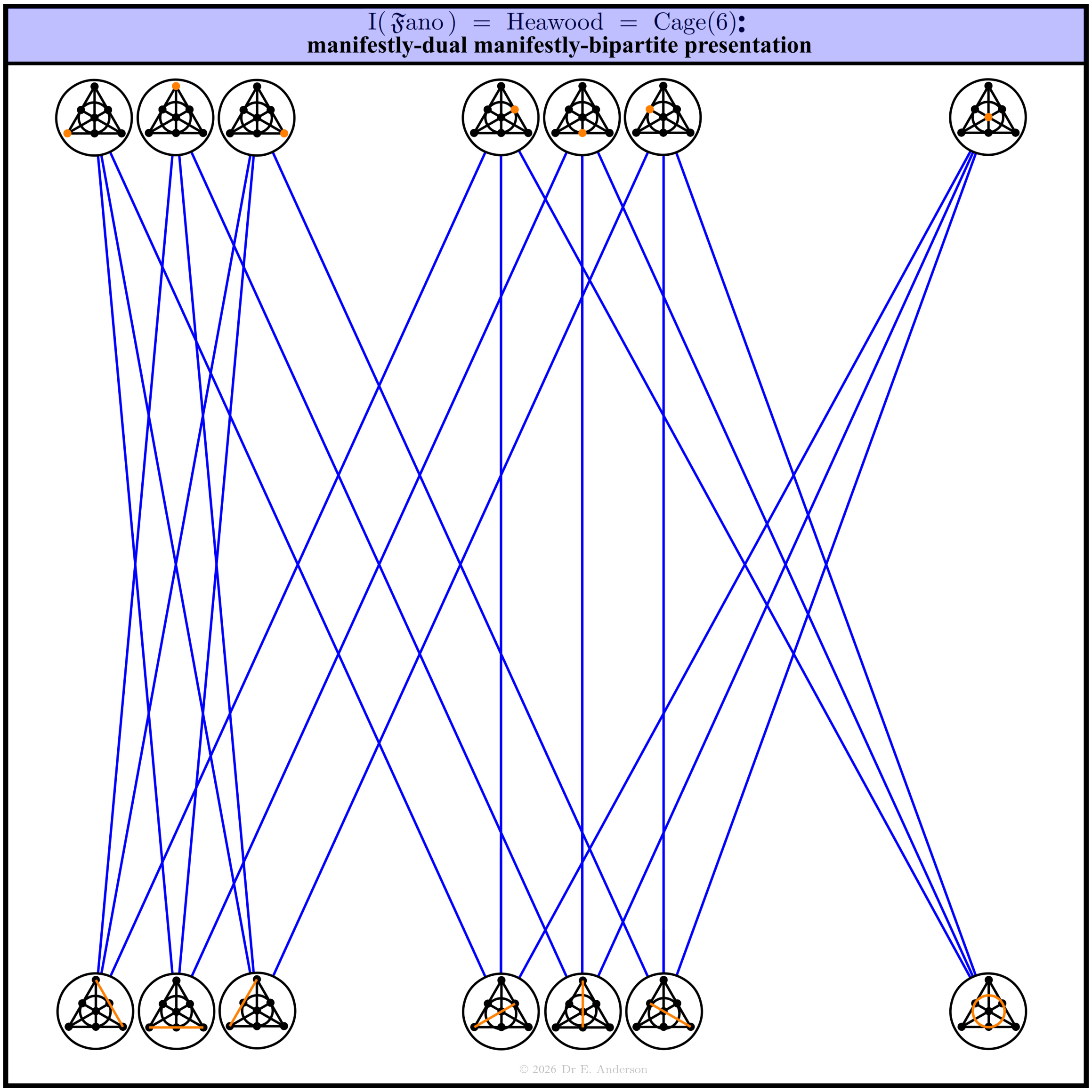

Figure 3:

few small objects, using nice presentations of the objects themselves is a favourable approach. This includes not restricting oneself to LaTeX's pre-defined symbols in such studies. This approach dates back at least to the 2000s among some Combinatorialists [37].

This is the approach taken in the current Encyclopaedia. Which has many further reasons to label graph, poset and other order structures' vertices by Combinatorial objects. For its principal objects of study are Combinatorial Arenas. I.e. Mathematical spaces, each modelling the totality of some kind of Combinatorial object. For many different small examples of types of Combinatorial object from basic Combinatorics. Or from discretely-representable parts of Linear Mathematics, Computer Science, Geometry, and Group Theory, and other parts of Abstract Algebra. Among all of which we find modelling of arenas by orders to be highly useful, with some simpler aspects already addressed by underlying graph models.

We also temporarily insert in-principle redundant and yet in practice zoomed-out bipartite colouring information. By giving 𝔉ano 's points' I(𝔉ano) vertices green backgrounds. The idea here is that even on a phone screen or in a low-resolution printout, one can still tell that the graph is bipartite. Without having to rely on zooming in or high enough printing resolution to reveal that these have but vertices highlighted in fireopal. To the others having edges emblazoned in fireopal.

Notational Remark 3 We next upgrade to the previous Article's [50] Fano call-signs in Fig 4. This amonts to truer-denoting the 2 parts by dots and clines. Which are visible enough to jettison the green backgrounds...

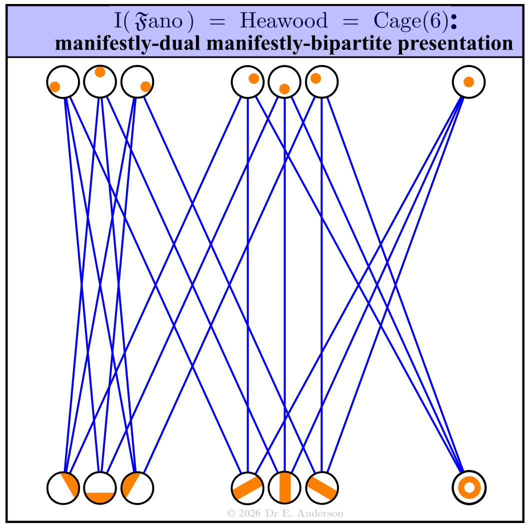

Figure 4:

1.4 Some basic counts

Remark 1 Having given one presentation so as to be able to display our graph, let us make the following basic counts for future use. Its number of vertices is

$$V(\,\mathrm{I}(\,\mathfrak{F}\mathrm{ano}\,)\,) \;=\; 14\;. \tag{1}$$

Its number of edges is

$$E(\,\mathrm{I}(\,\mathfrak{F}\mathrm{ano}\,)\,) \;=\; 21\;. \tag{2}$$

And its degree sequence is

$$\mathrm{deg}(\,\mathrm{I}(\,\mathfrak{F}\mathrm{ano}\,)\,) \;=\; 3^{14}\;. \tag{3}$$

Thus all of its vertices' degrees are the same; Graph Theorists call this *regular* [46]. And their common value is here 3 , which is called *cubic* by and much cherished by [2, 6, 10, 25, 47] Graph Theorists.

Remark 2 This 3 furthermore carries significance at the level of the Projecive configuration being modelled. In further detail, the underlying Projective configuration is 7_3. Signifying that 𝔉ano 's 7 points arranged to enjoy collinearity in 3 's. At the level of the incidence graph, then, this enforces the cubic subcase of regularity... While Projective-dually it involves 7 lines arranged to enjoy each meeting 3 other lines.

1.5 Bipartite graph implications

Remark 1 The 2 equal parts are of size 7 each. Given that the graph is cubic as well, we are talking about an incomplete bipartite graph. Were it complete, it would be

$$7 \;-\; 1 \;=\; 6\text{-regular}\;.$$

Remark 2

$$(\text{ uniformly-shared degree }) \;=\; 3 \;=\; \frac{6}{2} \;=\; \frac{(\text{ complete-homobipartite degree })}{2}\;.$$

Thus $I(\,\mathfrak{F}\mathrm{ano}\,)$ is a *half-complete* bipartite graph.

Among the p_3 Projective configurations, $\mathfrak{Fano}$ is the only one to enjoy this property. For, firstly,

$$\frac{p - 1}{2} = 3$$

is uniquely solved by

$$p = 7 .$$

And secondly, $\mathfrak{Fano}$ so happens to be the unique 7_3 Projective configuration [89].

Remark 3 See Sec 4 for some precise minimum and aesthetic properties of our particular choice of presentation in Fig 3.

1.6 Graph complement implications

Remark 1 There is little practical point to considering the complement $\overline{\mathrm{G}}$ of our graph G , since this has far more edges than our graph itself. This occurs whenever

$$E << E_{\mathrm{max}} = \frac{V(V - 1)}{2} .$$

For us,

$$E_{\mathrm{max}} = \frac{14 \times 13}{2} = 91 >> 21 = E . \tag{4}$$

So using $\overline{\mathrm{G}}$ to denote the complement of graph G ,

$$E\left(\overline{\mathrm{I}(\mathfrak{Fano})}\right) = 91 - 21 = 70 .$$

Exercise 1^{-} Check this number using regularity instead.

Remark 2 A finer consideration, for drawing and naming purposes, is to entertain whichever of G or $\overline{\mathrm{G}}$ is of smaller size ($=$ edge number). Which is to be gauged against the critical value

$$E_{\mathrm{crit}} := \frac{E_{\mathrm{max}}}{2} = \frac{V(V - 1)}{4} . \tag{5}$$

For us, this is

$$E_{\mathrm{crit}}(\mathrm{I}(\mathfrak{Fano})) = \frac{14 \times 13}{4} = \frac{91}{2} = 45.5 . \tag{6}$$

Then indeed

$$21 < 45.5 < 70 . \tag{7}$$

Thus we proceed with drawing, and naming, the 21-edge version!

2 A first few Graph-Theoretic properties

2.1 Structural analysis

Remark 1 I($\mathfrak{Fano}$) has no side-trees and is thus a cycle system alias foliation irreducible. It also has no vertices of degree 2, and so is a homeomorph irreducible. Thus it is a double irreducible: DI class D [49].

Remark 2 I($\mathfrak{Fano}$) is not however a cubeomorph irreducible, being rather a 5th cubeomorph of Tet .

2.2 Metric properties

Definition 1 Given a graph G, its *girth* $\gamma(\mathrm{G})$ is the length of its shortest cycle. While its *circumference* $c(\mathrm{G})$ is the length of its longest cycle. And its *diameter* $diam(\mathrm{G})$ is the maximum over all vertex pairs of the minimum lengths between each vertex pair. In each case length refers to path-length as measured by the number of edges in that path. By convention, an acyclic graph alias forest is assigned $\gamma = \infty$.

2.3 Traversibility properties

Remark 3 I($\mathfrak{Fano}$) is clearly not Eulerian. For by (3) it has all vertices of odd degree. But Eulerian graphs must have all vertices of even degree!

Remark 4 A widely used explicit Hamiltonian presentation is exhibited in our Cover-figure.

In this particular figure, we furthermore maintain vertex labelling by $\mathfrak{Fano}$ points and lines. By doing this, we are implicitly giving a map by which the first-principles bipartite incidence graph maps into this well-known presentation. Let us now upgrade this with Fano call-signs to form Fig 5.

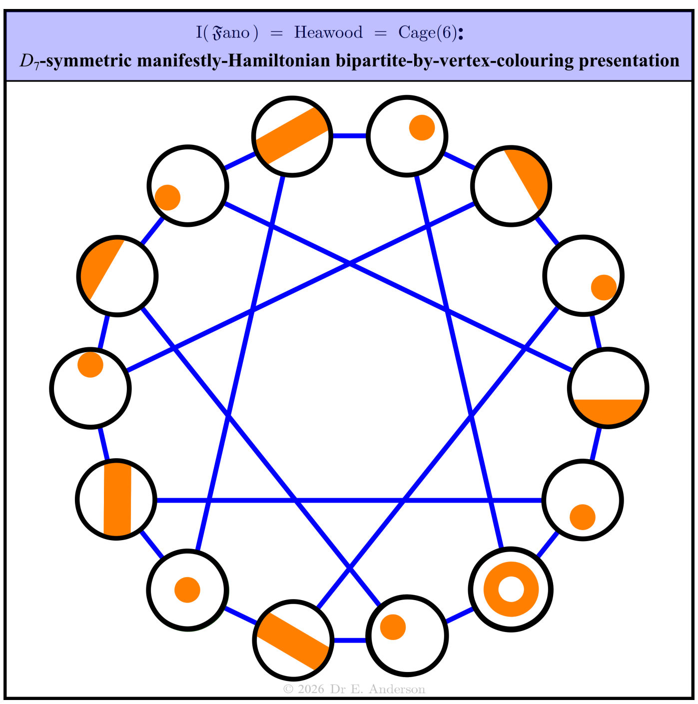

Figure 5:

Exercise 2 Show that

$$\gamma(\,\mathrm{I}(\,\mathfrak{F}\mathrm{ano}\,)\,) \;=\; 6\;, \tag{8}$$

$$d(\,\mathrm{I}(\,\mathfrak{F}\mathrm{ano}\,)\,) \;=\; 3\;. \tag{9}$$

Why are we not explicitly noting down $c(\,\mathrm{I}(\,\mathfrak{F}\mathrm{ano}\,)\,)$ in the current Article?

2.4 Symmetries

Remark 1 The Fano incidence graph has rather more symmetry than Fig 1's presentation managed to muster. Relative to $\mathfrak{F}$ano, $\mathrm{I}(\,\mathfrak{F}\mathrm{ano}\,)\,)$ has an extra bipartite-vertex colour-exchange symmetry, modelling Projective duality. Doubling the size of its symmetry group to [7]

$$|\,\mathrm{I}(\,\mathfrak{F}\mathrm{ano}\,)\,| \;\;=\;\; 168 \;\times\; 2 \;\;=\;\; 336\;.$$

In contrast, the cover figure presentation's symmetry group is just D_7 , of order 14 .

3 A minimum-crossing presentation

Remark 1 All presentations considered so far contain rather many crossings.

Exercise 3 Prove that $\mathrm{I}(\mathfrak{Fano})$ is nonplanar. Improve the bipartite presentation's crossings to 6 and then to 5. Next throw in some inner-face edges to the outer face in the manifestly Hamiltonian presentation so as to attain 4 crossings.

Remark 2 Fig 6 gives a further presentation with just 3 crossings.

$\mathrm{I}(\mathfrak{Fano}) = \text{Heawood} = \text{Cage}(6)$ **: minimum-crossing presentation**

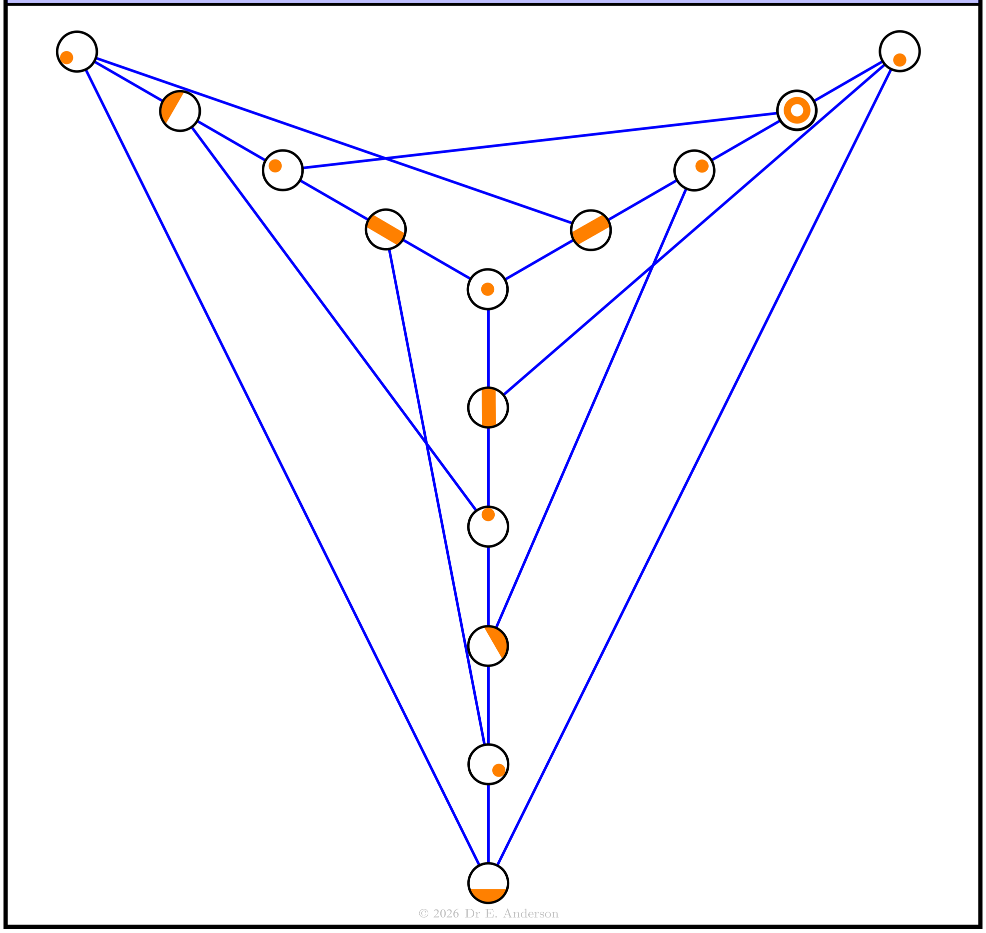

Figure 6:

Exercise 4 Combine this figure with exploitation of $\mathrm{I}(\mathfrak{Fano})$'s high girth to prove that in fact its crossing number

$$Cr(\mathrm{I}(\mathfrak{Fano})) = 3 .$$

Remark 3 Fig 6 is thus a crossing-number minimizing presentation.

4 Further presentational finery

4.1 Placing the bipartite graph in general position

Remark 1 Let us start by placing the vertices representing points uniformly on a line. With the vertices representing lines vertically beneath (Fig 7.a). Thus forming a 6×1 grid.

Remark 2 There are however a number of crossings not in general position.[1] I.e. ≥ 3 lines intersecting at other than a vertex. We mark these in grey. With 1 dot for the conflation of 3 crossings. And a with second ring for the conflation of 6 .

Remark 3 We next lengthen our integer grid to resolve increasing numbers of these. Alternatively attempting to increase the depth does not resolve these.

Remark 4 Suppose that we maintain the corner-point and mid-point block structure. In the sense of keeping each of these triples internally uniformly spaced. Then the minimum grid in general position is column 4's top entry: 11×1 .

Exercise 5$^-$ Does dropping the block groupings shorten this grid?

Remark 5 In our presentations, the vertex size is large enough that increasing the depth improves the clarity and aesthetics of one's figure. In the last entry of Fig 7, which we select for Fig 3 as well, we increase the depth as far as the square-grid presentation: 11×11 .

[1] E.g. at the time of writing this, [54]'s bipartite presentation fails to fully deal with this Topologically-adroit presentational feature.

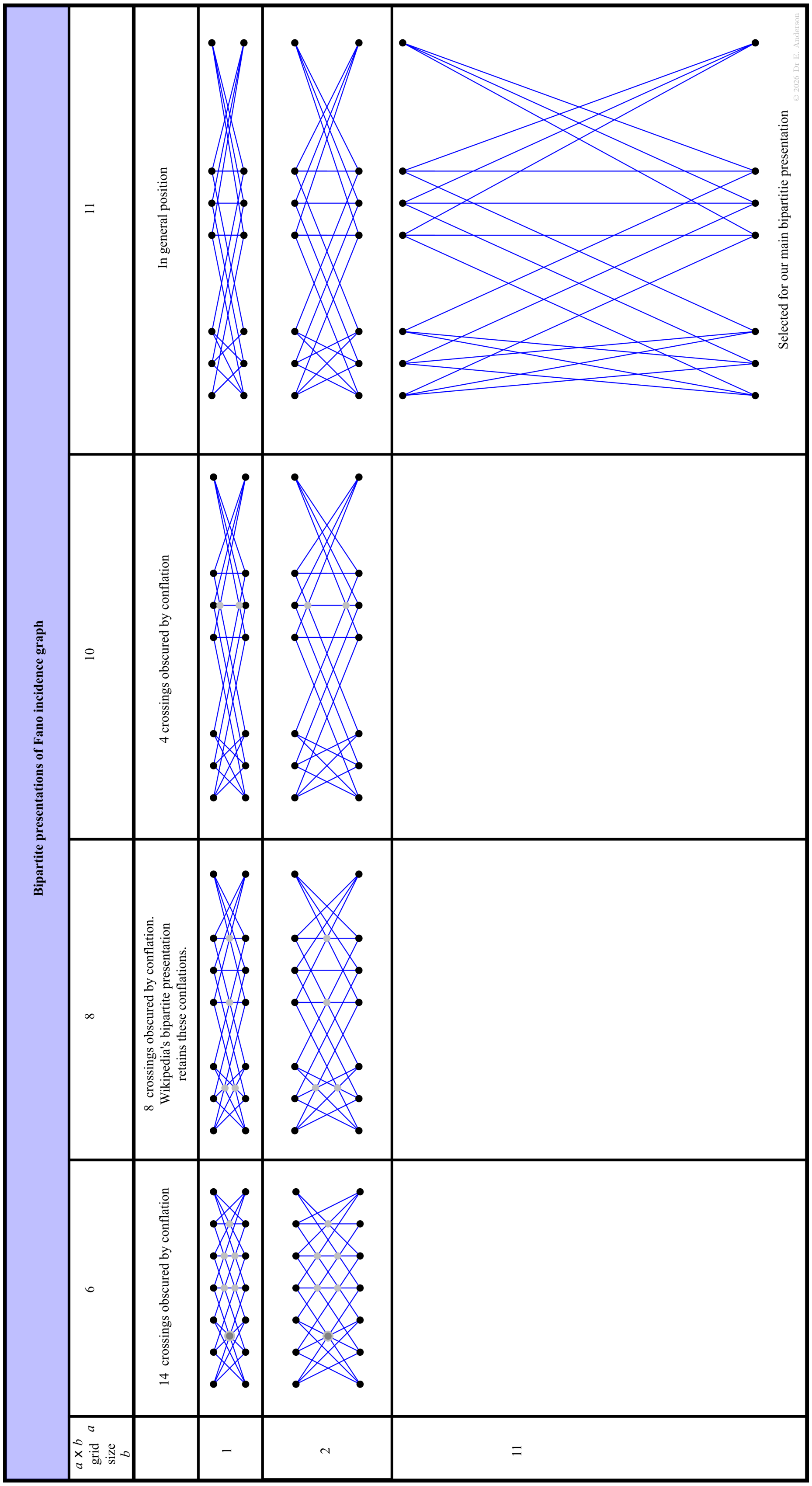
Bipartite presentations of Fano incidence graph
a x b grid size a b
6
8
10
11
14 crossings obscured by conflation
8 crossings obscured by conflation. Wikipedia's bipartite presentation retains these conflations.
4 crossings obscured by conflation
In general position
1
2
11
Selected for our main bipartitie presentation
© 2026 Dr E. Anderson

Figure 7:

4.2 Heptagonal shelling presentations

Remark 1 We first maintain the regular 14-sided polygon positions for the vertices. We find that keeping alternating edges and some vertex permutations permit formation of the annular structure indicated in Fig 8.a). This derives a presentation given in [55]. We now improve upon this in two different ways.

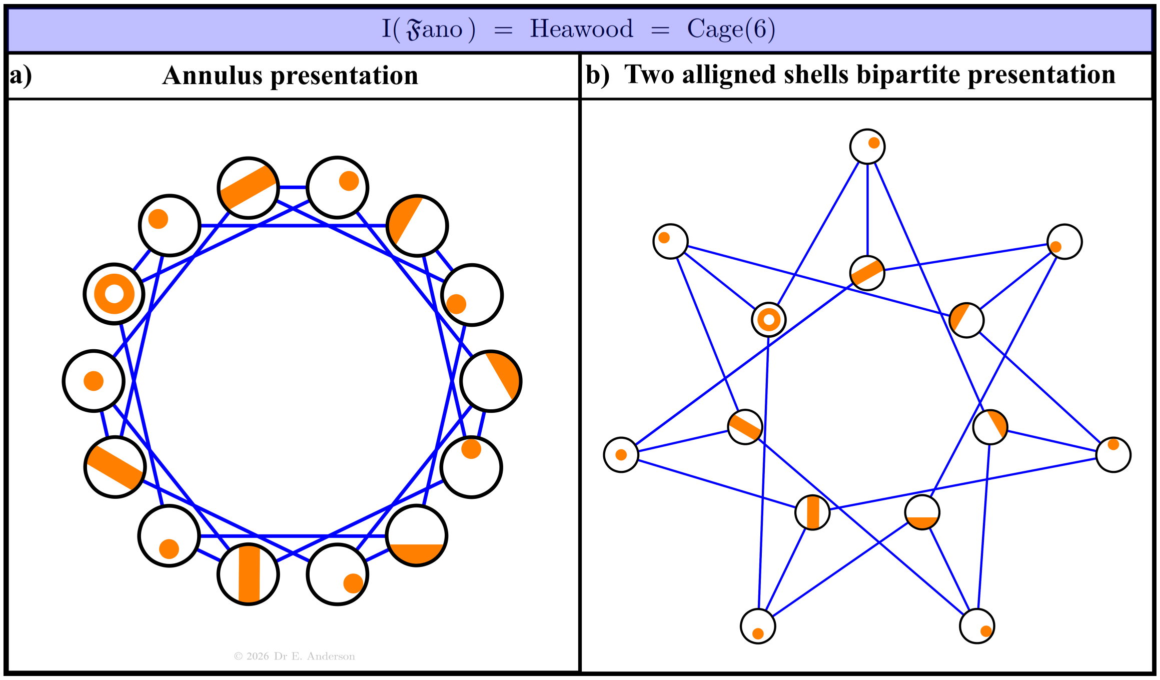

Figure 8:

Remark 2 We next keep the vertices representing points in position forming a regular heptagon. And move the vertices representing lines to form a second heptagonal shell both concentric with this and alligned with it . For our first placement, we take the 2 radii to be in a 2 : 1 ratio, yielding Subfig b)'s presentation.

Remark 3 Maintain the vertices representing points in a regular heptagon (Fig 9.a). We next choose another particular placing for a second concentric regular heptagon of Fano line vertices. Namely that which minimizes the edge-lengths subject to the side-condition of the heptagonal shelling. This no longer maintains alignment between the 2 concentric heptagons.

Perusing the previous figure, the connections pick out Subfig b)'s orange triangle's vertices as the ones that our Fano line vertex links to. We then construct outward-pointing equilateral triangles on each face in grey. And then link these by the pale grey lines to the opposite vertices. These pale grey lines intersect at the triangle's inner Fermat point F , cast in fuchsia. Which is where we place the line vertex so as to minimize the length of its 3 edges. Since the line vertices form a regular heptagon, this fixes all the remaining such vertices. We have thus minimized the totality of edge-lengths, yielding the presentation in Subfig c).

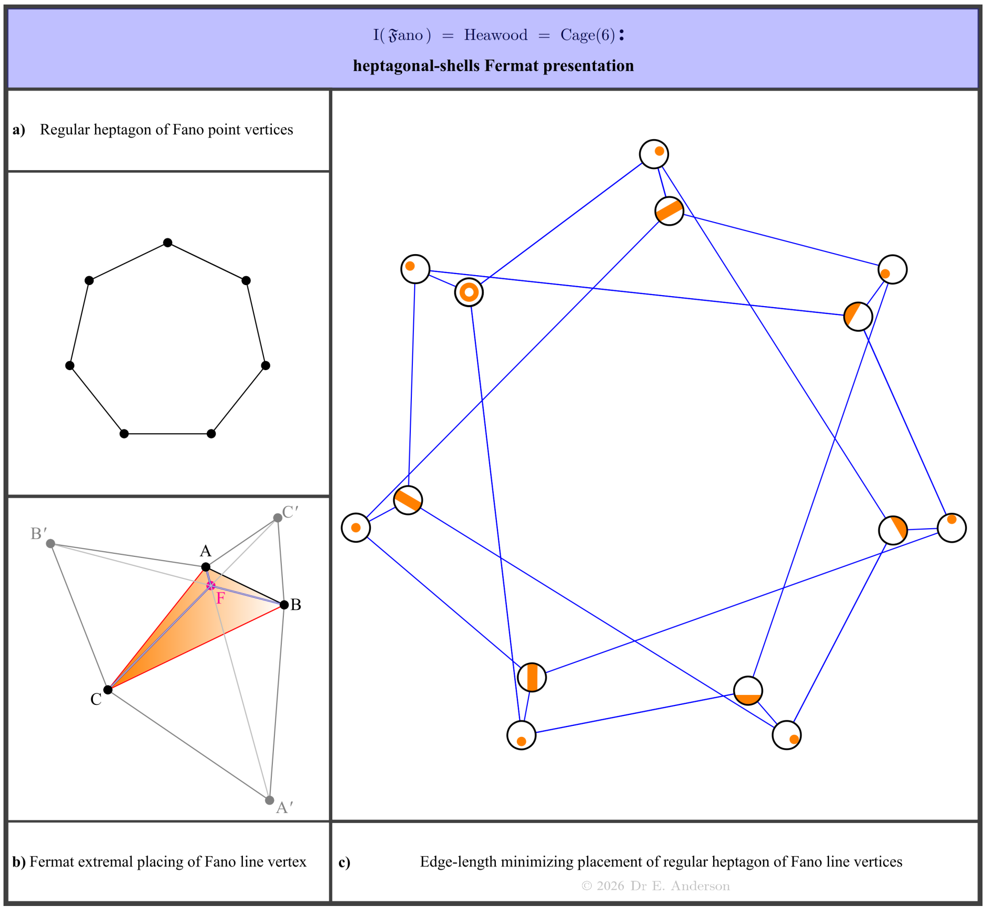

Figure 9:

Pointer D Whenever a bipartite graph admits an annulus presentation, it also admits one presentation per type of triangle centre. Around a dozen of which have basic meaning and are consequently also common knowledge. While orders of magnitude more of them can be found at [93]. Further selection principles may invalidate some of these from being used for a given bipartite graph. For instance circumcentres and Fermat points are capable of lying outside their triangles, which might not be one's goal when deploying 'centred Graph Drawing and Visualization'...

4.3 Unit-distance presentations

Remark 1 On the one hand, searching for such is straightforward to Geometrically pose and in principle to algorithmically carry out. On the other hand, actually obtaining solutions, detailing their diversity of features, and bounding or counting the extent of their non-uniqueness are not suitable matters for a basic introduction. For instance, 11 such are given in [38].

4.4 q-distance presentations

Remark 1 Let us here casually observe firstly that Figs 1 and 8.a) are 2-distance presentations.

Remark 2 While Figs 8.b) and 9 are 3-distance presentations. Which 3 is tied to the graph being cubic. And enjoying an $(f = 7)$-fold rotational symmetry of presentation. This provides a reason for q-distance presentations to cease to be a valuable feature for

$$q \geq \frac{E}{f} = \frac{21}{7} = 3$$

for our particular case of $\mathrm{I}(\mathfrak{Fano})$. This is a stronger bound than [53]'s, which returns

$$q \geq \left\lfloor \frac{N}{2} \right\rfloor = 7$$

for the current Article's graph. For sure, the $2 : 1$ ratio could be changed to any other real value without straying into $q \geq 4$. Where $\lfloor\ \rfloor$ denotes the floor function.

Open Question 1 More generally, q-distance presentations of graphs are not hitherto a standard topic in Graph Drawing and Visualization. Moreover, one should get a handle on up to which q-distance presentations remain of interest for a given graph parametrized by (V, E). With elements of structural regularity plausibly playing an aggravatory role when present.

5 Torus colorability and other properties

5.1 Exercise on some basics

Exercise 6$^-$ a) Show that the chromatic number

$$\chi(\mathrm{I}(\mathfrak{F}\mathrm{ano})) \;=\; 2\;.$$

And the edge-chromatic number

$$\chi(\mathrm{I}(\mathfrak{F}\mathrm{ano})) \;=\; 3\;.$$

b) Show that it is not *uniquely colourable* (see [50] for what this means).

5.2 The graphs and surfaces lemma

Lemma 1 Any graph with crossing number $\leq g$ can be embedded into a surface of genus g .

And into a non-orientable surface of genus $g - 1$.

Remark 1 This is by deforming the graph so that each hole can be used in isolation to resolve an individual crossing. With a non-orientability twist then being able to deputize for a hole.

Remark 2 There is consequently no interest in such embeddings (in the absence of further side-conditions that cannot always be guaranteed to hold).

Remark 3 One interesting question is what is the minimum genus g required to embed some particular graph. Or the minimum genus g required to do so into a non-orientable surface. These are not necessarily answered by Cr and $Cr - 1$. Since for some graphs, a hole or a twist can be used to deal with ≥ 1 crossing. In such cases, there may be some merit to the embedding.

Remark 4 Another stems from making the embedding Geometrically regular, in the sense exemplified below [7]

5.3 Heawood's presentation on the torus

Remark 1 The current Article's graph first arose in Heawood's work [1]. As an example of maximum possible number of colours for maps drawn on the torus $\mathbb{T}^2$, which is 7 .

Structure 1 The *Heawood map* demonstrating this is constructed as follows from regular hexagons. For a chunk of tessellation is to be involved. And regular hexagons are the smallest polygons to permit 6 nearest neighbours in a tessellation. So that if all of the nearest neighbours are forced to be coloured differently, these and the central hexagon together force 7 colours.

Incline a unit-side regular-hexagon tessellation of the plane. Relative to a hexagon of side $\sqrt{7}$. Through an angle of

$$\alpha \;=\; \arcsin\left(\frac{1}{2}\sqrt{\frac{3}{7}}\right)\;.$$

As per Fig 10.a).

Cast the large hexagon in the role of fundamental cell with the identification indicated in Subfig b). We then colour in the fundamental cell as in Subfig c). So as to establish that the violet hexagon has all 6 other colours of the rainbow as neighbours. This is sufficient to have a 7-colour map on $\mathbb{T}^2$.

One can also check that the central hexagon is not special in this way, by examining whichever peripheral hexagon.

Naming Remark 1 Hence the titular alias *Heawood graph* for the current Article's graph.

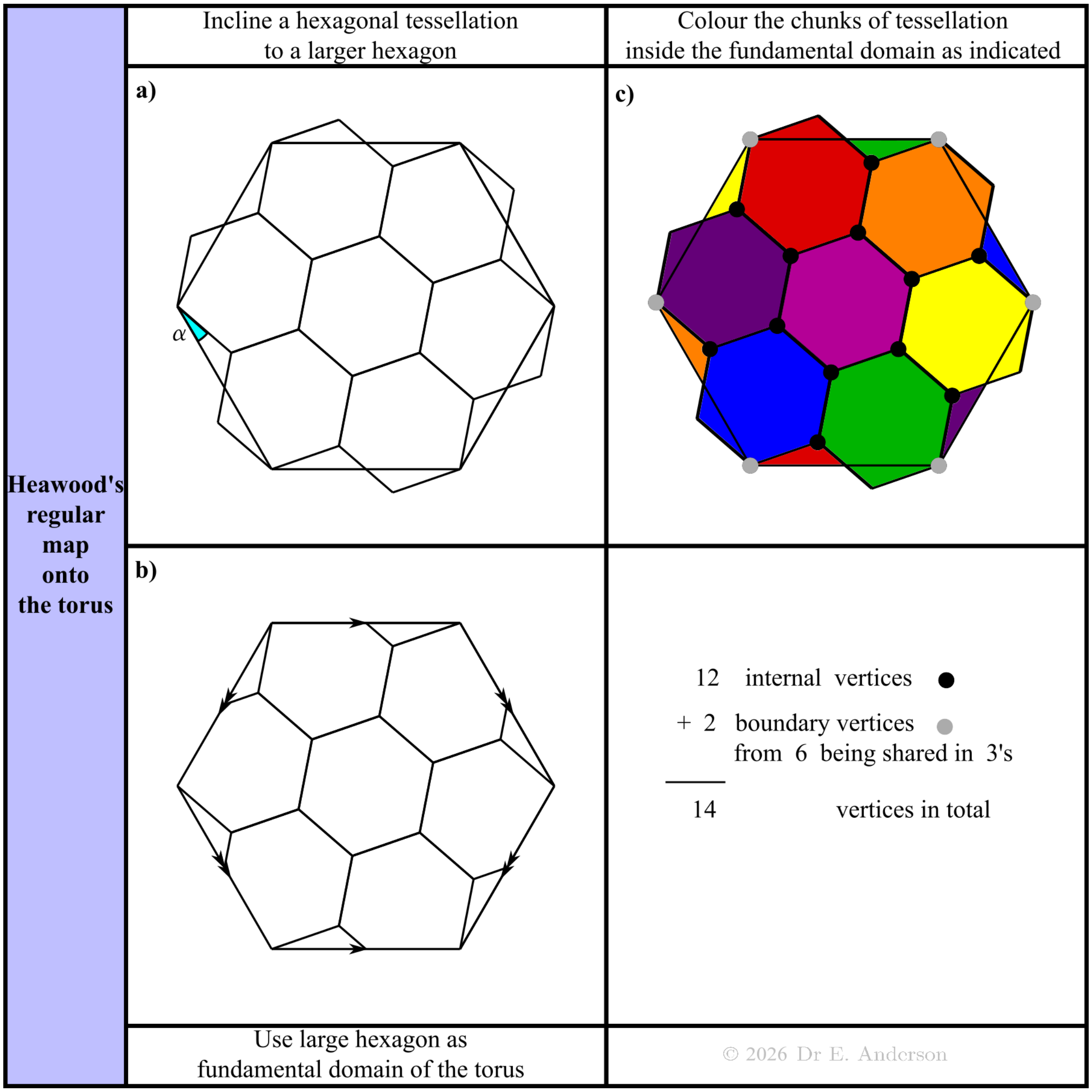

Figure 10:

Remark 2 Three reasons that this is interesting are as follows.

Firstly,

$$Cr(\text{Heawood}) \ = \ 3 \ > \ 1 \ = \ g\left(\mathbb{T}^2\right) \ .$$

Secondly, the above meets the definition of a regular map.

Thirdly, this map requires 7 colours. Serving in this way as a minimum counterexample to 6 colours sufficing for $\mathbb{T}^2$.

Exercise 7 a) Prove that Structure 1's angle and ratio are as stated.

b) Fill in the obvious gap by establishing that Structures 1 and 2's vertices indeed form the Heawood graph!

Exercise 8 Find the relative angle between the concentric regular heptagons in our Fermat presentation figure.

5.4 The barber's pole presentation

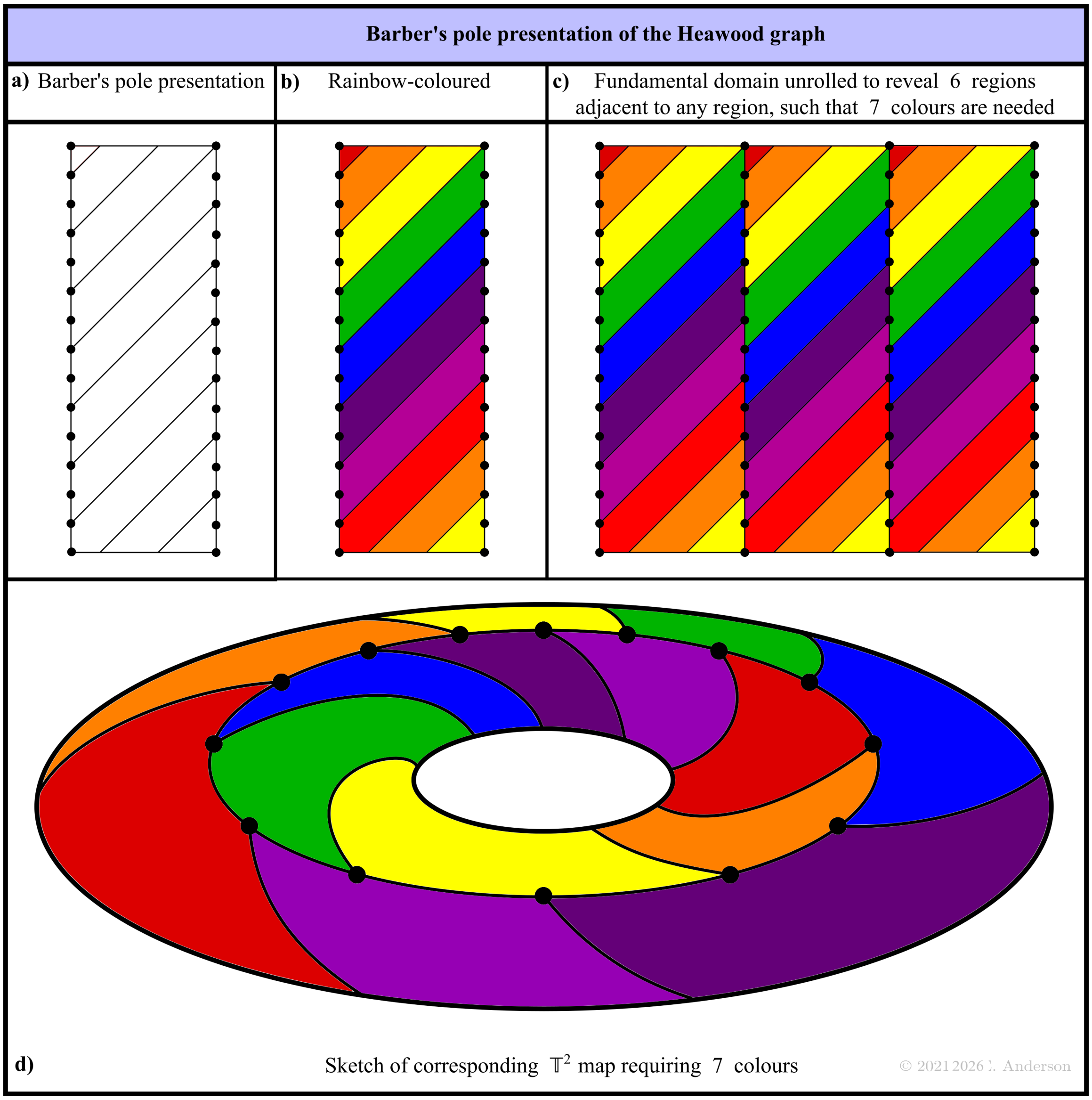

Figure 11:

Remark 1 In studying $\mathbb{T}^2$ itself, the above identification is not the simplest and most commonly encountered one. This is, rather, a square or rectangle: with just 2 labeling kinds of boundary-identification arrow. We thus also include the following presentation of the Heawood graph on $\mathbb{T}^2$ formed by a rectangular identification.

Structure 2 The 'toroidal barber's pole' presentation is given in Fig 11.a). Its $5 : 14$ aspect ratio is chosen so that the inclined lines are at a $\frac{\pi}{4}$-angle relative to the perimeter's sides.

This aspect ratio is rooted, firstly, the Heawood graph having 14 vertices, which we uniformly place on a vertical boundary line. Since the first features on both upper and lower boundaries, the vertical sides are 14 edges long. Secondly, we also make a second copy of our vertical boundary line. And inclinedly join the 2nd copy of the 1st vertex to the 1st copy of the 6th. The 2nd copy of the 3rd to the 1st copy of the 8th and so on. [Eventually you will need to use arithmetic $(\bmod\ 14)$.] So this inclined joining skips by $6 - 1 = 5$ vertices. So for the inclines to be at 45° to the sides, we need the short sides to be 5 edge-lengths apart.

Since the Heawood graph on $\mathbb{T}^2$ is 7-colourable as well, an even more vivid description is as follows (Subfig b). A *toroidal rainbow-coloured barber's pole*!

Remark 2 We then demonstrate that each region is indeed adjacent to the other 6 in this model by unrolling the fundamental domain into the plane in Subfig c). And end by presenting a view of $\mathbb{T}^2$ embedded in 3-d space bearing the 7-coloured Heawood graph in Subfig d). This has been selected to exhibit every region being adjacent to every other within the visible portion of $\mathbb{T}$ ... Vertex placement, and the position that the $\mathbb{T}^2$ is depicted to be viewed from, are of course highly nonunique.

5.5 The Heawood graph's toroidal polyhedron

Exercise 9 a) Embed $\mathrm{K}_5, \mathrm{K}_6$ and K_7 in $\mathbb{T}^2$.

b) Also show that the Geometrical dual of the Heawood polyhedron on the torus is K_7 .

Structure 1 The Heawood graph on $\mathbb{T}^2$ induces the *Szilassi polyhedron* in flat space. I.e. the only known polyhedron apart from the tetrahedron to have all faces adjacent. Its Geometrical dual K_7 correspondingly induces the *Császár polyhedron*. Which is the only known polyhedron apart from the tetrahedron to be bereft of diagonals.

Exercise 10$^-$ Explain why these two properties are Geometrically dual.

6 Cages

6.1 Definition

Definition 1 An (r, γ)-*cage* $\mathrm{Cage}(r, \gamma)$ [5, 26, 40] is an r-regular graph of a particular girth γ. Such that no r-regular graph on less vertices supports girth γ. Let us denote the most widely considered cubic cages by just $\mathrm{Cage}(\gamma)$.

Remark 1 This definition clarifies that cages are part of Extremal Graph Theory. Girth more generally plays a major role in Structural Graph Theory, and Projective Geometry.

6.2 Simple Examples

Exercise 11 a) Explain why cages for $r < 3$ are a trivial affair.

b) Prove that

$$\mathrm{Cage}(3) \; = \; \mathrm{Tet} \; .$$

$$\mathrm{Cage}(4) \; = \; \mathrm{Utilities} \; .$$

Example 0

$$\mathrm{Cage}(5) \; = \; \mathrm{Pet} \; :$$

the seminal graph depicted in Fig 12.

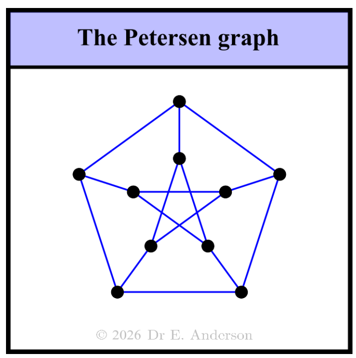

Figure 12:

For start with vertex 0 adjacent to $1, 2, 3$. None of these can be adjacent, since there would then be a 3-cycle. So 1 is adjacent to new 4 and 5. Were one of these adjacent to 2 or 3 as well, then there would be a 4-cycle. So 2 is adjacent to a distinct 6 and 7. And 3 is adjacent to a yet again distinct 8 and 9 (Fig 13.a). This forces

$$|\,\mathrm{Cage}(5)\,| \; \geq \; 10 \; . \tag{10}$$

Inspecting Fig 12, the Petersen graph indeed has girth $\gamma = 5$. Thus

$$|\,\mathrm{Cage}(5)\,| \; \leq \; 10 \; . \tag{11}$$

Together, (10, 11) yield that

$$|\,\mathrm{Cage}(5)\,| \; = \; 10 \; . \tag{12}$$

Thus the Petersen graph is a 5-cage.

It remains to establish uniqueness. nb n nnn The joint choice of edges $4\,6$ and $4\,8$ is licit. Picking an edge $4\,5$ is not licit by forming a 3-cycle. Nor is picking the edges $4\,6$ and $4\,7$ together, now by forming a 4-cycle. Thus the joint edge choice $4\,6$ and $4\,8$ is forced modulo relabelling. This then forces $5\,7$ and $5\,9$. And then $6\,9$ and $7\,8$. This forms the 'spiral galaxy' shape in Fig 13.b).

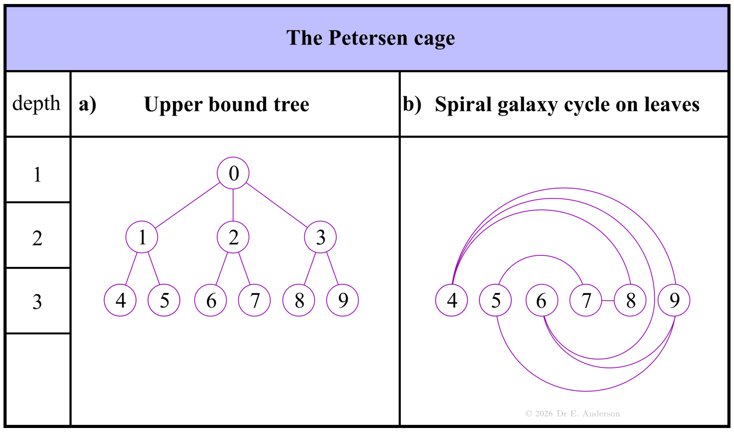

Figure 13:

The resulting graph is straightforwardly isomorphic to the Petersen graph.

Exercise 12$^-$ Reprove the first part by exhaustively checking that the cubic graphs on ≤ 8 vertices [53] contain no girth $\gamma = 5$ cases.

6.3 Heawood $=$ Cage(6)

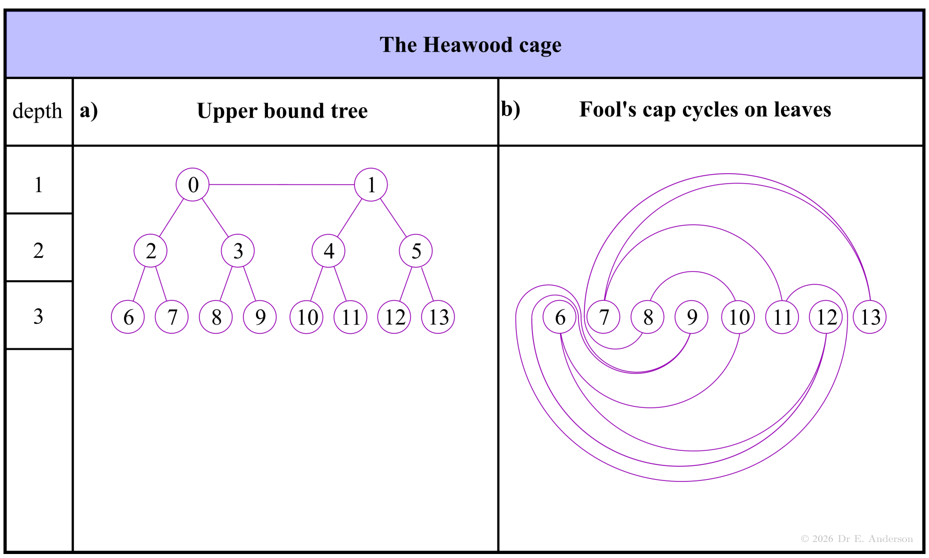

Figure 14:

Example 1.A) Let us first naïvely re-run Example 0 above. Then some of $4, 5, 6, 7, 8, 9$ can have a shared descendant S. Since say $0\,1\,4\,S\,6\,2$ is a 6-cycle, which is allowed. We just need 4 and 6 not to share a parent...

B) We can however avoid this even-γ obstruction by placing 2 vertices on the top floor, say labelled 0 and 1. Let 0 be adjacent to $2, 3$. Which are forced to be distinct from the $4, 5$ adjacent to 1. This works 1 floor further down as well (Subfig b). Which brings in 8 further vertices. Thus

$$|\,Cage(6)\,| \;\geq\; 14\;. \tag{13}$$

Upon inspection, $\mathrm{I}(\,\mathfrak{Fano}\,) = $ Heawood indeed has girth $\gamma = 6$. So

$$|\,\mathrm{Cage}(6)\,| \;\leq\; 14\;. \tag{14}$$

Together, (13, 14) yield that

$$|\,\mathrm{Cage}(6)\,| \;=\; 14\ . \tag{15}$$

Thus $\mathrm{I}(\,\mathfrak{Fano}\,) \;=\; \mathrm{Heawood}$ is furthermore a 6-cage.

C) Let us next establish that $\mathrm{I}(\,\mathfrak{Fano}\,) \;=\; \mathrm{Heawood}$ is the unique 6-cage, so as to confer a third major alias, $\mathrm{Cage}(6)$.

Maintaining girth 6 forms the following 'fool's cap' shape (Fig 14.b) on the leaves of the above tree. Modulo initial labelling choices, the following is enforced. 6 has edges to 10 and 12 . 7 to 11 and 13 . 8 to 10 and 13 . And 9 to 11 and 12 .

Remark 1 Observe that Exercise 12's exhaustion is already substantially outclassed in this case, in particular as regards the uniqueness part of the proof. For now one would have to find and check the girths of the 509 [56, 34] cubic graphs on 14 vertices...

6.4 The above existence method is rooted on the Moore bound

Remark 1 Example 1 is along similar lines to [33]. Which then proceeds to apply the the previous Subsec's method B) without filling A)'s logical gap.

Remark 2 [33] also displays superposed analogues of a)-and-b). In contrast, we visually decompose each graph's figure into a tree part a) and a cycle part b).

Remark 3 That a tree plays a role follows from combining trees being acyclic with high girth forbidding shorter cycles. So the extended neighbourhood of 1 or 2 initial – height-1 – points is a tree.

Remark 4 This tree vertex-count part of the argument readily generalizes to arbitrary γ and r . So the previous two Subsecs' uses of trees are not 2 one-off tricks. But rather the odd- and even-γ variants of a single systematically reuseable method which can be attempted for every cage.

Pointer 0 The corresponding tree vertex-count bound on cage orders is called the *Moore bound* [12, 40]. For cubic graphs, this takes the following form.

$$|\,\mathrm{Cage}(\gamma)\,| \;\geq\; \begin{cases} 1 \;+\; 3\sum_{i\,=\,0}^{\frac{\gamma\,-\,3}{2}} 2^i & \gamma \text{ odd} \\ \qquad\; 2\sum_{i\,=\,0}^{\frac{\gamma\,-\,2}{2}} 2^i & \gamma \text{ even}\ . \end{cases} \tag{16}$$

In this context, Pet has

$$10 \;=\; 1 \;+\; 3\,(\,1 \;+\; 2\,)\ .$$

While Heawood has

$$14 \;=\; 2\,(\,1 \;+\; 2 \;+\; 2^2\,)\ .$$

Remark 5 The Moore bound is a bound for the following reason. In general, it does not return the size of the cage, but rather just a lower bound on it. Cases in which the two coincide are called *Moore cages*.

Exercise 13$^-$ a) Find the general-r version of this tree vertex count.

b) Simplify your generalization, and consequently (16), by use of your knowledge of geometric progressions.

6.5 Arenas of cages declared

Structure 1 Let

$$\mathfrak{C}\text{age}$$

denote the arena of all cages.

$$\mathfrak{N}\text{ontrivial}\mathfrak{C}\text{age}$$

the arena of nontrivial cages.

$$\mathfrak{M}\text{oore}\mathfrak{C}\text{age}$$

the arena of nontrivial cages whose Moore bound is tight. And

$$\mathfrak{K}\text{nown}\mathfrak{C}\text{age}$$

the arena of known cages to date. Use the prefix $\mathfrak{C}$ubic to restrict to the cases in which cubic cages alone are being entertained.

A priori,

$$\mathfrak{C}\text{age} \;=\; \mathbb{N}_0 \;\times\; \mathbb{N}_2 \;.$$

Where the second factor is indexed $\infty, 3, 4, 5, \ldots$. As somewhat awkward inheritance from the standard convention that we stated under the definition of girth.

While

$$\mathfrak{N}\text{ontrivial}\mathfrak{C}\text{age} \;=\; \mathbb{N}_3 \;\times\; \mathbb{N}_5 \;.$$

This corresponds to the standard view that whichever of $r \leq 2$ and $\gamma \leq 4$ holding render a cage trivial.

Exercise 14$^-$ a) Complete justifying this by extending Exercise 11.b-c) by finding

$$\text{Cage}(\,3,\,r\,) \;\;\text{and}\;\; \text{Cage}(\,4,\,r\,) \;\;\forall\;\; r \;\geq\; 3 \;.$$

6.6 The cycle part of the decomposition

Remark 1 The cycle part in the decomposition that we depict is not just a standard presentation of a cycle for the following reason. Its vertex order is rather constrained by the tree and its height function. Following our nose for Graph Drawing and Visualization [42], we uncross the cycles. This is in part aided by the decomposition itself cutting down on presentational crossing numbers. And leads to our new presentations, alongside our names for them: spiral galaxy and fool's cap.

7 Conclusion

7.1 A citizen of Kallista

Remark 1 As indicated by its multiple names corresponding to its arising along multiple conceptually-distinct lines of thought in multiple Mathematical subjects,

$$\mathrm{I}(\mathfrak{Fano}) \quad = \quad \mathrm{Cage}(6) \quad = \quad \mathrm{Heawood}$$

is a citizen of Kallista [45, 46, 94].

Remark 2 The first is an Incidence Geometry [81, 92] alias Block Design Theory [76, 91] and Hypergraph Theory [29] name. Celebrating the Fano configuration $\mathfrak{Fano}$ itself lying at the root of this triple confluence of lines of thought. Our graph is furthermore derived from this by forming the corresponding incidence graph, conferring some Incidence Geometry bias. $\mathfrak{Fano}$ is a fortiori a homodual Projective configuration. And not only a Projective plane but also the minimum such. In this way, the current Article's corresponding incidence graph has Projective-Geometric content.

Remark 3 The second name refers to a structural extremization property in Graph Theory. It is moreover no coincidence that this minimum property coincides with the incidence graph resulting from the minimum Projective plane. While it is additionally a Moore cage: a rather rare property that renders some cages rather easier to find and study.

Remark 4 The third name refers to a graph colorability property. Minimumly establishing the necessity for $\mathbb{T}^2$ to have a 7-colour theorem analogue of the plane's 4-colour theorem. This is the historical context in which Heawood first found and studied this graph.

Remark 5 As is typical for citizens of Kallista, multiple heirs ensue. Though let us first map out its ancestors.

7.2 The Heawood graph's pedigree

Remark 1 Heawood is the child of the union of two of the most exhalted citizens of Kallista known to date. Namely the above Fano configuration $\mathfrak{Fano}$ and Graph Theory's most significant known graph: the Petersen graph, Pet .

Remark 2 A weaker connection between Pet and Heawood is that both are cubic. Furthermore, both are cubeomorphs of the first cubeomorph-irreducible graph: the tetrahedron graph, Tet . And Heawood is a second cubeomorph of Pet .

Exercise 15 Find 1 copy of Pet hiding inside our Cover-figure upon performing 2 reductive cubeomorphs.

Remark 3 A stronger connection is that Pet is the 5-cage while Heawood is the 6-cage. So Heawood is Pet 's cage heir. Even more strongly, both are Moore cages. So Heawood is furthermore Pet 's Moore cage heir.

Pointer 1 ⟨3⟩ Another route from Tet to Pet is as follows. First increase Platonic solid face size from 3 to 4 to 5 . This yields the dodecahedron. View this as a tessellation of $\mathbb{S}^2$. Antipodally identifying $\mathbb{S}^2$ produces $\mathbb{RP}^2$. And restricting this to the marked dodecahedron returns Pet . This is the additional 'backflip' included in Fig 16. In the sense that m goes from 2 to 4 to 10 and then back to 5 .

Exercise 16 Check this antipodal identification of the dodecahedron. Also show that antipodal identification of 3-d's other 4 Platonic solids is uneventful.

Pointer 2 ⟨3⟩ See [53, 60] respectively for first outlines of Tet and Pet as citizens of Kallista. Furthermore, [50] documented how $\mathfrak{Fano}$ is also a direct heir of Tet . As the completion of Tet 's

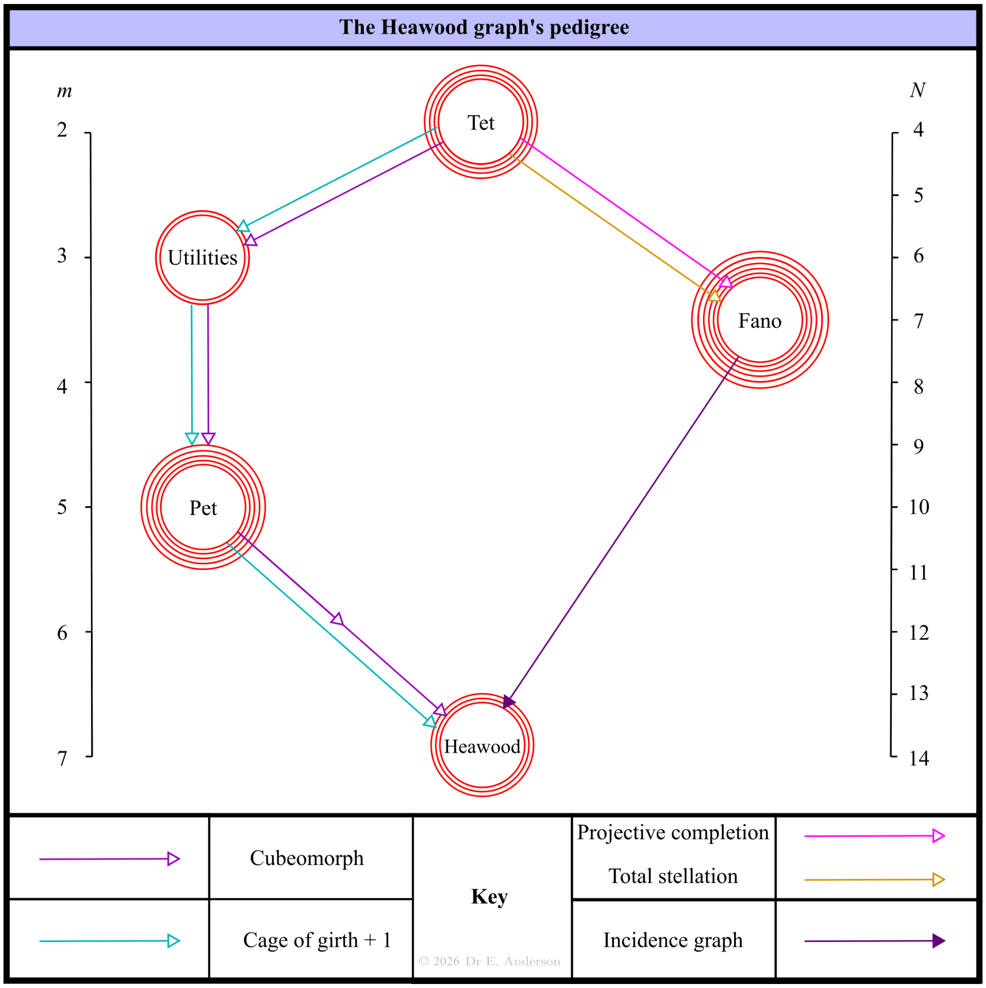

Figure 15:

alter ego as the smallest Affine plane to the smallest Projective plane. And as its first stellation, or the next Apollonian network from a Contact Geometry point of view.

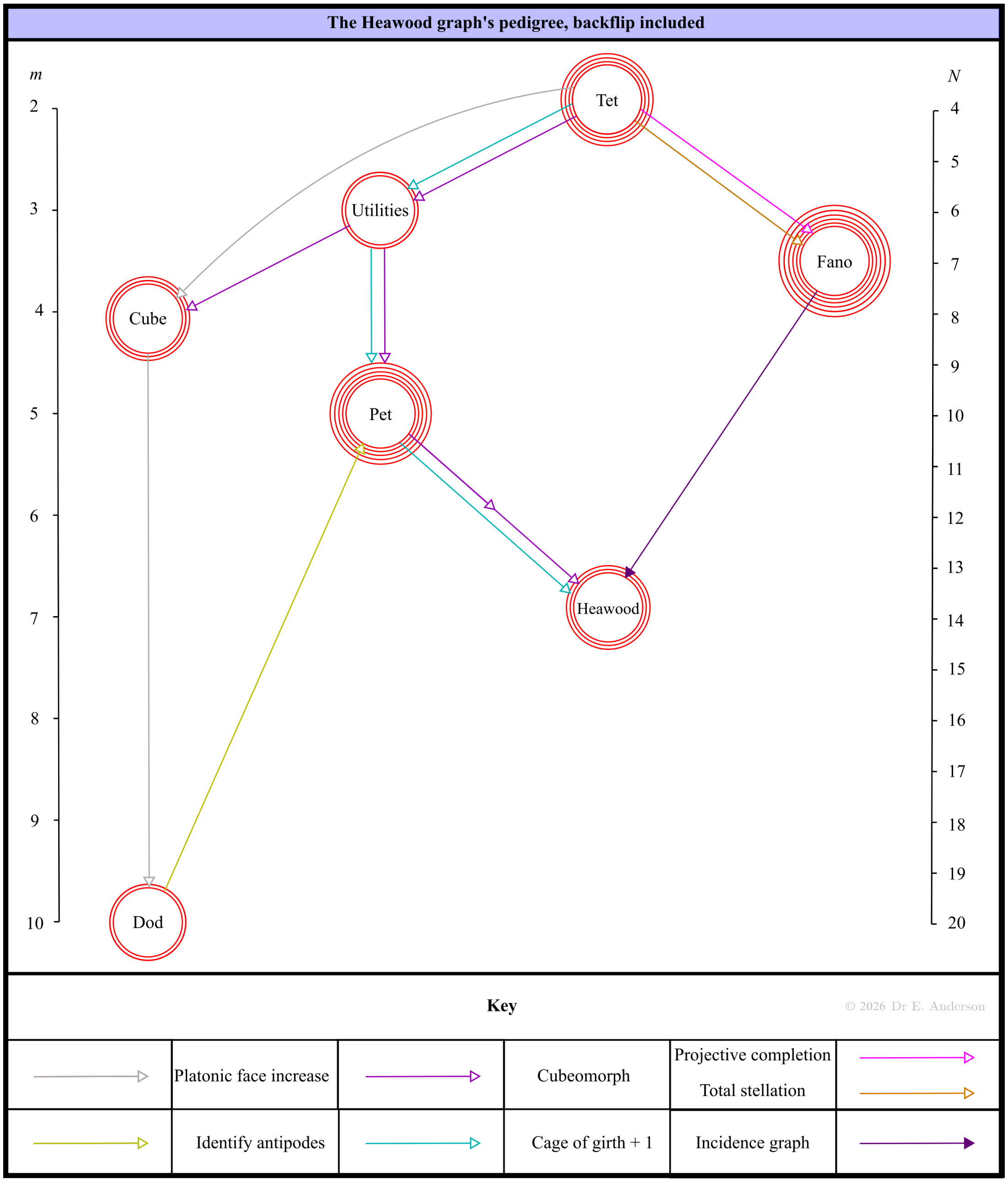

The Heawood graph's pedigree, backflip included
m
N
Tet
Utilities
Fano
Cube
Pet
Heawood
Dod
2
3
4
5
6
7
8
9
10
4
5
6
7
8
9
10
11
12
13
14
15
16
17
18
19
20
Key
© 2026 Dr E. Anderson
Platonic face increase
Cubeomorph
Projective completion
Total stellation
Identify antipodes
Cage of girth + 1
Incidence graph

Figure 16:

7.3 Cage heirs

7.3.1 Cubic cages

Theorem 1[2] Among the nontrivial cages, only

$$\gamma = 5, 6, 8, 12$$

can be Moore.

Remark 1 This restriction suffices for Moore cages to be non-generic.

Proposition 2 All cubic cages that can be Moore, are.

Remark 2 Thus, while Heawood is Pet 's cubic plain-and-Moore heir, Heawood itself has distinct such.

Pointer 3 ⟨5⟩ Its cubic cage heir is the *McGee graph* Cage(7) on $m = 12$.

Pointer 4 But its cubic Moore cage heir is the *Tutte* 8-*cage* [5] Cage(8) alias *Tutte–Coxeter graph* [9, 8, 30] ⟨5⟩.

While the *Tutte* 12-*cage* [30] Cage(12) alias *Benson graph* [14]. ends this line, as the maximum cubic Moore cage ⟨7^+⟩.

These are on $m = 15$ and 63 respectively. Both of these are themselves exhalted citizens of Kallista.

7.3.2 General-r cages

Proposition 2 Among the $\gamma = 5$ nontrivial cages, only $r = 3$ and 7 are Moore.

Remark 1 ⟨6⟩ So suppose that not γ but r is increased. Then Pet itself has distinct plain and Moore cage heirs. Respectively the *Robertson cage* [13] Cage(5, 4) on 19 vertices.

And the *Hoffman–Singleton cage* [12] Cage(5, 7) on 50 .

Pointer 5 Heawood does however manage to have a unique cage heir in this sense. Namely the *Wong cage* [26] Cage(6, 4) on 26 vertices ⟨6⟩. Its generic – not-Moore – heir is the *O'Keefe–Wong cage* [24] Cage(6, 7) on 90 vertices ⟨8⟩.

Exercise 17 a) Generalize the Moore bound count to arbitrary r .

b) Efficiently show that McGee, Robertson and O'Keefe–Wong do not match the Moore bound's count. While the two Tuttes, Wong and Hoffman–Singleton do.

Remark 2 At the level of arenas, we have so far pinned matters down to

$$\mathfrak{Moore}\mathfrak{Cage} \subseteq \mathbb{N}_3 \times \{ 5, 6, 8, 12 \} .$$

[2] This and the next SSSec use conceptually neat portions [45] of a Moore cage characterization theorem [40] originally attributed to [20, 21] ⟨6-7⟩.

7.3.3 Generalizing the non-tree part of the Moore split

Remark 1 The cycle part of Sec 6's split in a sense generalizes to higher r. It is moreover capable of causing further cages to depart from the Moore bound of [40]. This is why we use $\subseteq$ rather than $=$. Since this phenomenon does not affect the cubic Moore cages, we make no further mention of it.

Exercise 18 Use some of the smaller cages that you found in Exercise 14 to figure out what happens to the non-tree part of the cage for $r \geq 4$.

Pointer 6 This feeds into how some of the

$$\gamma = 6, 8, 12$$

cages fail to be Moore. Via the generalization of the cycle part of the split being capable of preventing a Moore bound cage from existing.

7.3.4 Nonunique cages

Proposition 3 Moore cages are unique.

Pointer 7 $\langle 7^+ \rangle$ The not-Moore $\text{Cage}(9)$ however turns out to be nonunique. This is the minimum cubic example, sporting precisely 18 solutions, on $m = 29$.

Nonuniqueness recurs for $\text{Cage}(10)$, now with multiplicity 3, on $m = 35$.

While the example with smallest vertex number – 30 – is $\text{Cage}(5, 5)$, with multiplicity 4. Though this one is an heir of Pet, not of Heawood.

Remark 1 This leaves us with a temporary arena-level error to correct. I.e. that cage arenas are not Cartesian grids of cases, or subsets thereof. But are rather *multi-sets* thereover. Meaning that some (r, γ) coordinate values can carry multiple entries for a point.

7.3.5 Known cages

Open Question 2 In fact, humanity has not succeeded in finding any cubic cages beyond the Moore maximum $\gamma = 12$.

Remark 0 For on the the one hand, Moore cages are easier to find. Unfortunately there are not very many of these. And yet a tree-removing ansatz of Balaban's [19] reduces the Tutte cages to the 7- and 11- cages [59]. With a separate one-off trick of Tutte's [15] obtaining the first of these from the Möbius–Kantor incidence graph (Sec 7.4.1). [Not that McGee required either trick to obtain the 7-cage!]

While on the other hand, finding the 9 and 10 cages is harder [18, 22, 23]. As is establishing the exact multiplicity of their nonuniqueness and that the 11-cage is unique [27, 32, 35].

Remark 1 A first part of the subsequent problem is that graphs, even regular graphs, rapidly become numerous enough not to be exhaustively findable, even with advanced computer assistance.

Remark 2 A first advance is to sandwich the possible sizes of cages by complementing the Moore bound below with some other bound above. Which role was first played by the *Erdös bound* [16, 40]. The interval between the two is however large for all unknown cubic cages (and more generally) $\langle 6 \rangle$.

While some improved bounds have since been found [40] $\langle 7^+ \rangle$, the intervals between the two remain large. Rendering brisk progress in the cubic cage-finding venture unlikely [45].

7.4 Some Projective Geometry heirs

7.4.1 Homodual Projective configuration heirs

Recollection 1 The Fano Projective configuration is $\mathfrak{F}\text{ano} = 7_3$: with 7 points collinear in 3's. It is furthermore homodual: also with 7 lines coinciding in 3's. And not only the minimum Projective configuration but also the minimum Projective plane.

Pointer 9 ⟨3-4⟩ If homoduality is to be retained and yet Projective-planarity can be sacrificed, then there is a unique proxime involving 8 points. This is *the Möbius–Kantor configuration* 8_3 [85]

$$\mathfrak{MK} = 8_3 .$$

The corresponding *Möbius–Kantor (incidence) graph*

$$\mathrm{I}(\mathfrak{MK})$$

on $m = 8$ is an heir of the Heawood graph.

Exercise 19 Our Fermat style of presentation is reuseable for all homodual Projective configurations' incidence graphs. Construct it for $\mathrm{I}(\mathfrak{MK})$.

Pointer 10 The Pappus [51, 83, 85] and Desargues [57, 85] configurations play further fundamental roles in Projective Geometry. As marked by Pappus' theorem and Desargues' theorem holding in the usual Euclidean plane, and playing fundamental structural roles [71, 68, 84] . ⟨2-4⟩.

And by abstract planes in finite Projective Geometry being qualified as (non-)Desarguian [82] and pp. 719-727 of [92] $\langle 5-7 \rangle$.

The Pappus and Desargues Projective configurations lie 1 and 2 points past Möbius–Kantor respectively. By which stage projective configurations have become persistently nonunique. So we are talking about one of the 3 9_3's and then one of the 10 10_3's [89].

The corresponding incidence graphs

$$\mathrm{I}(\mathfrak{P}\text{appus}) \text{ and } \mathrm{I}(\mathfrak{D}\text{esargues})$$

[52, 58] are heirs of the Heawood graph via its sole proxime $\mathfrak{MK}$. On $m = 9$ and 10 respectively.

7.4.2 Projective Geometry heirs

Pointer 11 ⟨4⟩ We now instead find the heir to $\mathfrak{F}\text{ano}$ viewed as a Projective plane. Or find the heir to $\mathfrak{T}\text{et}$ viewed as an Affine plane, and then complete it.

The following condition is Algebraically necessary for an Affine plane to exist. It must contain

$$\mathrm{d}_{\mathrm{AP}} := n^2 \text{ points for } n \in \mathbb{N}_2 .$$

$n = 2$ supports the minimum Affine plane

$$\mathfrak{T}\text{et} = \mathfrak{M}\text{AP} ,$$

containing

$$|\,\mathfrak{T}\text{et}\,| = 2^2 = 4 \text{ points} .$$

Which also complies with further line number and point-line incidence conditions as outlined in [50].

While $n = 3$ supports 1 *proxime Affine plane*

$$\mathfrak{H}\text{esse} = \mathfrak{P}\text{AP} ,$$

containing

$$|\mathfrak{Hesse}| = 3^2 = 9 \text{ points} .$$

The corresponding necessary condition for a Projective plane to exist is as follows [73]. It must contain

$$\mathrm{d_{PP}} := n^2 + n + 1 \text{ points for } n \in \mathbb{N}_2 .$$

points. $n = 2$ supports the minimum Projective plane

$$\mathfrak{M}\mathrm{PP} = \mathfrak{Fano}$$

with

$$|\mathfrak{Fano}| = 2^2 + 2 + 1 = 7 .$$

While $n = 3$ supports 1 *proxime projective plane*

$$\mathfrak{p}\mathrm{PP} = 13_4 .$$

With

$$|\mathfrak{p}\mathrm{PP}| = 3^3 + 3 + 1 = 13 .$$

The 4-subscript indicates that it attains collinearity-and-coincidence in 4's. Rendering its incidence graph on $m = \mathrm{d_{PP}} = 13$ quartic: $r = 4$. This incidence graph is then another Heawood heir:

$$\mathrm{I}(\mathfrak{p}\mathrm{PP}) = \mathrm{I}(13_4) .$$

Pointer 12 We just outlined severe and swift limitations on existence, uniqueness and known cases for cages: plain and Moore. So it is balanced to leave our Readers aware that Projective planes come with rather comparable limitations.

⟨6⟩ $n = 6$ is minimum, past Fano's $n = 2$, to have no Projective plane exist. This corresponds to

$$m = \mathrm{d_{PP}} = 6^2 + 6 + 1 = 43$$

points.

⟨7⟩ While $n = 9$ is the minimum for nonuniqueness. Corresponding to

$$m = \mathrm{d_{PP}} = 9^2 + 9 + 1 = 91$$

points. With multiplicity 4 . The ensuing diversity also manages to capture the following two minimum features.

3 of these Projective planes are non-Desarguian.

Finally a first heterodual pair of Projective planes is realized thereamong : the *Hall pair* [65].

Open Question 3 At present $n = 12$ is the first entirely unsettled case, corresponding to

$$m = \mathrm{d_{PP}} = 12^2 + 12 + 1 = 157$$

points. At least some instances of projective planes are known past this point.

Remark 1 The main known no-go for Projective planes is as follows. ⟨7⟩

Theorem 2 (Bruck–Ryser) [66]. There are no Projective planes if the following both hold.
i)

$$n = 1 \text{ or } 2 \pmod 4 .$$

ii)

$$n \neq i^2 + j^2 \text{ for any } i, j \in \mathbb{N}_0 .$$

Remark 2 Within these restrictions, Heawood picks up a suite of further corresponding incidence graph descendants on

$$m = \mathrm{d_{PP}} = n^2 + n + 1 .$$

7.4.3 The Cremona–Richmond configuration

Pointer 13 ⟨6⟩ This $\mathfrak{C}$R is one of the 15_3's : with 15 points collinear in 3's [61, 85]. It is furthermore homodual.

A first distinctive feature is that it contains the Petersen graph while maintaining its 5-fold symmetry. In fact expanding from

$$Sym(\text{Pet}) = S_5$$

to

$$Sym(\mathfrak{C}\text{R}) = S_6 \ .$$

In this way, $\mathfrak{C}$R is a second child of note arising from the union of Fano and Petersen.

A second is that $\mathfrak{C}$R is the minimum Projective configuration to sport girth $\gamma = 4$ [62]. This eventually led to the truer name-and-notation *minimum generalized quadrangle*, $\mathfrak{M}$GQ . Affording both a generalized quadrangle extension [75] and a broader generalized n-a-gon extension (see the next SSSes). It is also consequently the minimum Projective configuration to support poset orders [45] (for triangles are forbidden in these [46]).

A third is that the corresponding incidence graph is

$$\text{I}(\mathfrak{C}\mathfrak{R}) = \text{Cage}(8) = \text{Tutte-8} \ .$$

7.4.4 And beyond

Pointer 14 This starts a recurring pattern according to which

$$\gamma(\, I(\mathfrak{p}\text{C})\,) = 2\,\gamma(\mathfrak{p}\text{C}) \ .$$

The minimum $\gamma = 6$ and 8 cases are particularly strong citizens of Kallista as well.

The first of these returns the *generalized hexagon* $\mathfrak{g}$H of Cayley and Tits [67]. For which

$$\text{I}(\mathfrak{g}\text{H}) = \text{Tutte-12} = \text{Cage}(12) = \text{MaxMooreCage} \ .$$

While girth 8 yields the *generalized octagon* $\mathfrak{g}$O of Tits and Ree [67]. By this point, we are out of Moore cages:

$$\gamma = 8 \times 2 = 16 > 12 \ .$$

Yet $\mathfrak{g}$O satisfies other maximal properties, such as minimaxing out the following.

Theorem 3 [Feit–Higman] [70]. Finite generalized polygons can only exist for

$$\gamma = 3, 4, 6, 8 \ .$$

7.5 Graph colouring generalizations

7.5.1 Heawood's map-colourability bound on surfaces

Remark 1 Sec 5's 7-colourability of $\mathbb{T}^2$ generalizes as follows ⟨4⟩.

Heawood bound For the colouring of maps on genus-g surfaces, the following number of colours is sufficient.

$$\chi(g) = \left\lfloor \frac{7 + \sqrt{48\,g + 1}}{2} \right\rfloor . \tag{17}$$

Where $\lfloor\ \rfloor$ denotes the floor function.

Exercise 20 a)$^-$ Work out $\chi(g)$ for $\mathbb{S}^2$, $\mathbb{T}^2$ and the 2-holed torus ${\mathbb{T}_2}^2$.

b) Prove the Heawood bound (17).

7.5.2 The Franklin graph

Pointer 15 The corresponding necessity conditions were eventually worked out [17].

One case fails necessity: the Klein bottle $\mathbb{K}^2$ – genus $g = 1$ non-orientable – is not 7- but 6-colourable.

With the *Franklin graph* [3] serving as minimum counterexample ⟨5⟩.

In terms of m , this is a precursor to Heawood : 6 versus 7 . But in terms of $\mathbb{K}^2$ having greater Topological complexity than $\mathbb{T}^2$, it is an heir.

7.5.3 No known Szilassi or Császár polygon heirs

Exercise 21 a) Prove that the following is a necessary condition for a polyhedron on a genus-g surface not to have any diagonals.

$$12\,g = (V - 3)(V - 4) . \tag{18}$$

With dual statement that the following is a necessary condition for an all-faces-adjacent polyhedron on a genus-g surface to exist.

$$12\,g = (F - 3)(F - 4) . \tag{19}$$

b) b) Reconcile this with the tetrahedron, Szilassi and Császár examples *at the level of counting*.
c) Find the next 3 smallest Combinatorial solutions (for all that these are not known to Geometrically support any such polyhedra).

Pointer 16 Observe that K_5 and K_6 are embeddable on $\mathbb{T}^2$ (Exercise 9) and yet no diagonal-free polyhedron is said to ensue from them. This indicates that there is more to the Császár polyhedron than just the above count. And dually likewise for the Szilassi polyhedron. For instance, they require realization within $\mathbb{R}^3$ with flat faces, which carries further Geometrical content ⟨6⟩.

Exercise 22 Find the next 3 values of g admitting Combinatorial solutions – in $\mathbb{N}$ – of (18) or (19).

Open Question 4 However, *no* further polygons embeddable in $\mathbb{R}^3$ with flat faces obeying either the no-diagonals or the all-faces-adjacent properties are known.

7.6 The Coxeter graph as a further heir

Exercise 23 Show that the Heawood graph possesses 28 6-vertex cycles.

Exercise 24 a) Find 7 copies of Pet graph within Heawood .

b) Find 84 copies!

Exercise 25$^+$ Show that each 6-cycle is disjoint from precisely 3 others. One of which is the symmetric difference of the other 2 .

Pointer 17 ⟨6⟩ Represent each 6-cycle by a vertex. Assign an edge to each disjoint pair. This returns the *Coxeter graph* [28] on $m = 14$.

7.7 Diagrams of the Heawood graph's heritage

7.7.1 A fairly full account, at least nearby

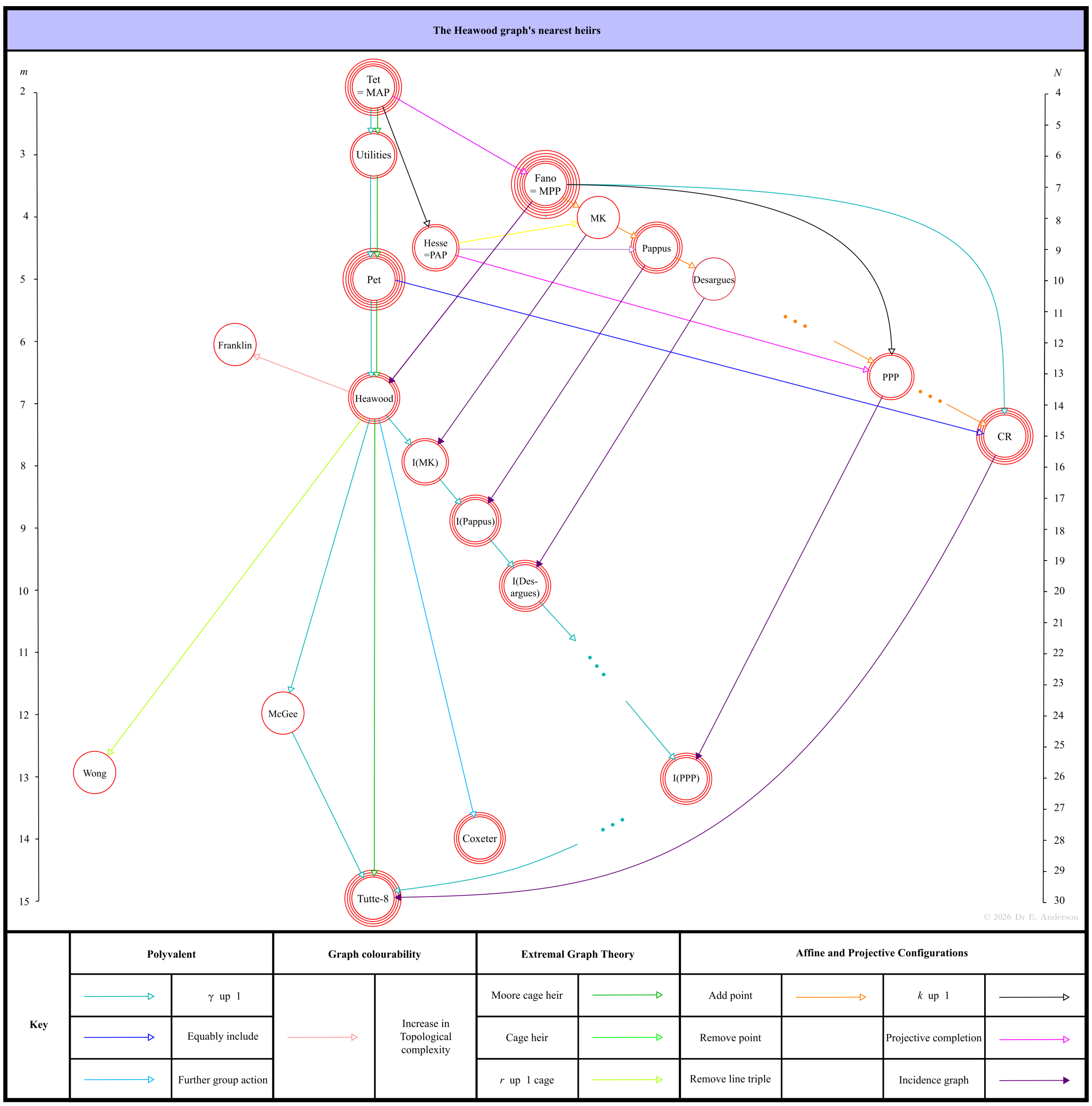

Figure 17:

Remark 1 We plot heirs on 12 to 30 vertices in Fig 17.

7.7.2 The big 5

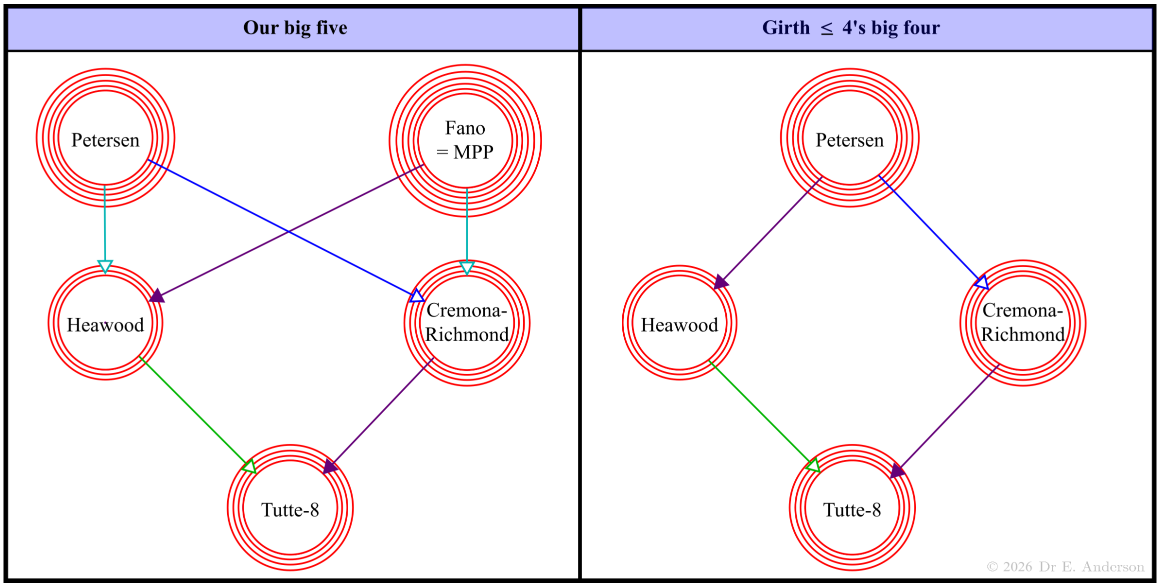

Figure 18:

Remark 1 Next we pick out 5 of the most significant objects in Fig 18.a). Any model containing 2 parents producing 2 children cannot however be a lattice. For this is the *crossed square*: a forbidden subposet in lattices [46]. And this applies to $\mathfrak{Fano}$ and Pet having Heawood and $\mathfrak{C}\text{R}$ as children.

Remark 2 With Fano containing triangles – forbidden subgraphs in a poset's graph skeleton, one approach is to remove $\mathfrak{Fano}$. By restricting modelling solely to the girth ≥ 4 portion of $\mathfrak{K}\text{allista}$. Then Subfig b)'s model ensues, which is the simplest nontrivial poset and furthermore a lattice.

7.7.3 A longer-range selection

Remark 1 A larger selection of some of the most significant citizens is in Fig 19.a). This picks the incidence-graph, next-Moore and next-Feit–Higman for its arrow relations. Subfig b) cuts down to the next-even-Moore arrow, which in particular removes Petersen from contention. Subfig c) additionally cuts down to the relatively-significant even-generalized p-gons. Which in particular removes $\mathfrak{Fano}$ from contention as well. While Subfig d) expands a) by using the next-Moore arrow. Finally Subfig e) restricts d) to girth $\gamma \geq 4$.

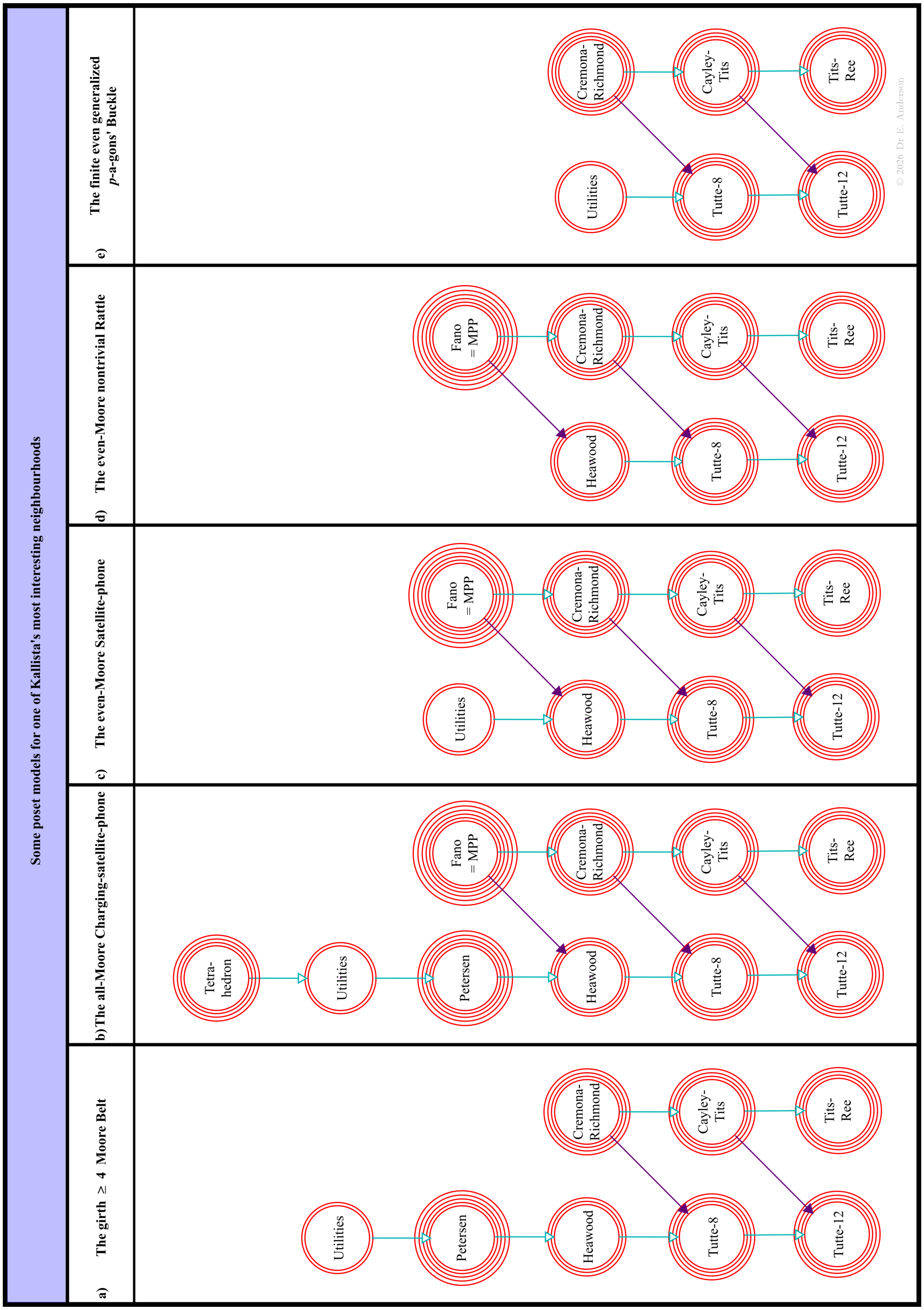
Some poset models for one of Kallista's most interesting neighbourhoods
a) The girth ≥ 4 Moore Belt
Utilities
Petersen
Heawood
Tutte-8
Tutte-12
Cremona-Richmond
Cayley-Tits
Tits-Ree
b) The all-Moore Charging-satellite-phone
Tetra-hedron
Utilities
Petersen
Heawood
Tutte-8
Tutte-12
Fano = MPP
Cremona-Richmond
Cayley-Tits
Tits-Ree
c) The even-Moore Satellite-phone
Utilities
Heawood
Tutte-8
Tutte-12
Fano = MPP
Cremona-Richmond
Cayley-Tits
Tits-Ree
d) The even-Moore nontrivial Rattle
Heawood
Tutte-8
Tutte-12
Fano = MPP
Cremona-Richmond
Cayley-Tits
Tits-Ree
e) The finite even generalized p-a-gons' Buckle
Utilities
Tutte-8
Tutte-12
Cremona-Richmond
Cayley-Tits
Tits-Ree
© 2026 Dr E. Anderson

Figure 19:

7.7.4 The Cremona–Richmond heresies

Remark 1 S. Sánchez [45] called Subfigs 18.b) and 19.c) and e) the *Cremona–Richmond heresies*. This is because they have no place for the elsewise-mighty $\mathfrak{Fano}$: a precursor for so much of Discrete Mathematics. Among these, 19.c) is the *great Cremona–Richmond heresy.* In which the titular configuration supplants both the $\mathfrak{Fano}$ 'god' of Discrete Mathematics and the Petersen 'god' of Graph Theory. While 19.e) supports further acknowledgment of Petersen as parent of Cremona–Richmond. By being free – unmenaced by crossed squares – to reissue 18.b)'s blue arrow. Yielding a further picture fully extending Subfig 18.b).

Remark 2 Some further motivation for considering higher girth is the powerful theory of the generalized N-gons itself. And the major role of girth 4 and 5 in the theory of snarks [39]: probably the most complex tribe descending from the Petersen graph. These matters, as well as Order Theory, explain why S. Sánchez developed the theory of *girtheomorphs.* I.e. homeomorphs (or cubeomorphs, etc.) that are furthermore girth-preserving.

Open Question 5 To what extent is there an analogue of the modern Discrete Mathematics that flows from $\mathfrak{Fano}$. Whose objects have girth $\gamma \geq 4$ and thus flows instead from the Cremona–Richmond configuration $\mathfrak{C}$R ?

And again for minimum girths $\gamma = 5, 6, 7$ and 8 . With initial particular interest in the even girths among these. For Feit–Higman reasons, with 8 in particular being the top Feit–Higman value.

Remark 3 A further idea here [45] is that girth-4 permits unification of the $\mathfrak{Fano}$ family with the remaining major branch of modern Combinatorics: Order Theory [98, 96, 95, 100, 99, 97]. But this would only be a reasonably full unification if the girth $\gamma \geq 4$ versions of the $\mathfrak{Fano}$ heirs are comparably nice, diverse and broadly applicable to the originals. So one would need to see how Projective configurations, Projective planes, designs, matroids, ensuing finite Group Theory (etc) do in this regard [45]. With an eye open for further lines of heir that only become possible with girth ≥ 4. While also bearing in mind that this is not the only possible means of unification. Given that, for instance, Garrett Birkhoff [95] was able to more subtly pair each finite Projective Geometry with a lattice.

Previous work along similar lines includes [74, 79, 89, 80, 87] and, with higher girth, [67, 89, 86].

Acknowledgments I thank S. Sánchez and A. Ford for discussions, as per [50]. And the Applied Combinatorics and Topology Discussion Group members.

References

[1] P.J. Heawood, “Map-colour Theorem". Quart. J. Math. **24** 322 (1890).

[2] R.M. Foster, “Geometrical Circuits of Electrical Networks", Trans. Amer. Inst. Elect. Eng. **51** 309 (1932).

[3] P. Franklin, “A Six Color Problem", J. Math. Phys. **13** 363 (1934).

[4] F.W. Levi, *Finite Geometrical Systems* (U. Calcutta, Calcutta 1942).

[5] W.T. Tutte, “A Family of Cubical Graphs", Proc. Cambridge Philos. Soc. **43** 459 (1947).

[6] R. Frucht, “Graphs of Degree Three with a given Abstract Group", Can. J. Math., **1** 365 (1949).

[7] H.S.M. Coxeter, “Self-Dual Configurations and Regular Graphs." Bull. Amer. Math. Soc. **56** 413 (1950); reprinted as one of the essays in *The Beauty of Geometry. 12 Essays* (Southern Illinois U.P. 1968; Dover, Mineola N.Y. 1999).

[8] W.T. Tutte, “The Chords of the Non-ruled Quadric in $PG(3,3)$ ", Can. J. Math. 10: 481 (1958).

[9] H.S.M. Coxeter, ibid. 484, with even the same title!

[10] W.T. Tutte, “On the Symmetry of Cubic Graphs", Can. J. Math. **11** 621 (1959).

[11] W.F. McGee, “A Minimal Cubic Graph of Girth Seven" Can. Math. Bull. **3** 149 (1960).

[12] A.J. Hoffman and R.R. Singleton, “On Moore graphs with diameters 2 and 3 , IBM J. Res. Develop. **4** 497 (1960).

[13] N. Robertson, “The Smallest Graph of Girth 5 and Valency 4 ", Bull. Amer. Math. Soc. **70** 824 (1964).

[14] C.T. Benson, “Minimal Regular Graphs of Girth Eight and Twelve", Canad. J. Math **18** 1091 (1966).

[15] W.T. Tutte, *Connectivity in Graphs* (U. Toronto P., Toronto 1966).

[16] P. Erdös, A. Rényi, and Vera T. Sós, "On a Problem of Graph Theory" Studia Sci. Math. Hungar., **1** 215 (1966).

[17] G. Ringel, and J.W.T. Youngs, “Solution of the Heawood Map-coloring Problem". Proc. Nat. Acad. Sci. U.S.A. **60** 438 (1968).

[18] A.T. Balaban, “A Trivalent Graph of Girth Ten" J. Combin. Theory **B** **12** 1 (1972).

[19] “Trivalent Graphs of Girth Nine and Eleven and Relationships among the Cages", Rev. Roumaine Math. **18** 1033 (1973).

[20] E. Bannai and T. Ito, “On Finite Moore Graphs", J. Fac. Sci. Tokyo, **20** 191 (1973).

[21] R.M. Damerell, “On Moore Graphs", Proc. Cambridge Phil. Soc. **74** 227 (1973).

[22] N.L. Biggs and M.J. Hoare, “A Trivalent Graph with 58 Vertices and Girth 9 , Discrete Math. **30** 299 (1980).

[23] M. O'Keefe and P-K. Wong, “A Smallest Graph of Girth 10 and Valency 3 . J. Combi Theory **B** **29** 91 (1980).

[24] “The Smallest Graph of Girth 6 and Valency 7 , J. Graph Theory **5** 79 (1981).

[25] H.S.M. Coxeter, R. Frucht, and D.L. Powers, *Zero-Symmetric Graphs: Trivalent Graphical Regular Representations of Groups* (A.P., New York 1981).

[26] P-K. Wong, “Cages - A Survey" J. Graph Theory **6** 1 (1982).

[27] “On the Smallest Graphs of Girth 10 and valency 3 ", Discrete Math. **43** 119 (1983).

[28] H.S.M. Coxeter, “My Graph", Proc. London Math. Soc. **46** 117 (1983).

[29] C. Berge “Hypergraphs: Combinatorics of Finite Sets" (Elsevier 1984).

[30] A.E. Brouwer, A.M. Cohen and A. Neumaier, *Distance Regular Graphs* (Springer-Verlag, New York 1989).

[31] D.A. Holton and J. Sheehan, *The Petersen Graph* (C.U.P., Cambridge 1993).

[32] G. Brinkmann, B.D. McKay and C. Saager, “The Smallest Cubic Graphs of Girth Nine", Combinatorics, Probability and Computing, **4** 317 (1995).

[33] V.K. Balakrishnan, *Graph Theory* (McGraw–Hill, New York 1997).

[34] R.C. Read and R.J. Wilson, *An Atlas of Graphs* (O.U.P., New York 1998).

[35] B.D. McKay, Wendy Myrvold and J. Nadon, “Fast Backtracking Principles applied to find New Cages", in 9th SODA Conference Proceedings (1998).

[36] C. Godsil and D. Royle, *Algebraic Graph Theory* (Springer-Verlag, New York 2001).

[37] J-L. Loday and María O. Ronco, “Order Structure on the Algebra of Permutations and of Planar Binary Trees", J. Algebraic Combin. **15** 253 (2002), arXiv:math/0102066.

[38] E.H-A. Gerbracht, “Eleven Unit Distance Embeddings of the Heawood Graph." http://arxiv.org/abs/0912.5395.

[39] G. Brinkmann, J. Goedgebeuer, J. Hägglund and K. Markström, “Generation and Properties of Snarks" J. Combi. Theory. **B 103** 468 (2013), arXiv:1206.6690 .

[40] G. Exoo and R. Jajcay, “Dynamic Cage Survey" Elec. J. Combi. **DS13** (2013).

[41] A.T. White, “Graphs and Finite Geometries", in *Handbook of Graph Theory* 2nd ed., ed. J.L. Gross, J. Yellen and P. Zhang (Chapman and Hall, Boca Raton Fl. 2014).

[42] *Handbook of Graph Drawing and Visualization* ed. R. Tamassia (Taylor & Francis, Boca Raton, Fl. 2014).

[43] C. Buchheim, M. Chimani, C. Gutwenger, M. Jünger and Petra Mutzel “Crossings and Planarization", in [42].

[44] T. Nishizeki and M.S. Rahman, “Rectangular Drawing Algorithms", in [42].

[45] Combinatorial and Geometrical discussions between E.A. and S. Sánchez (2018-2020). Some involved A. Ford.

[46] E. Anderson, *Applied Combinatorics*, Widely-Applicable Mathematics Series. A. Improving understanding of everything with a pinch of Combinatorics. **0**, (2022). Made freely available in response to the pandemic here: institute-theory-stem.org/combinatorics/ .

[47] M. Conder and P. Potočnik, “Census of Cubic Edge-Transitive Graphs" https://fostercensus.graphsym.net/ (2025).

[48] Online Encyclopaedia of Applied Graph and Order Theory, institute-theory-stem.org/online-encyclopaedia-of-graphs-and-orders/ .

[49] E. Anderson and A. Ford (she/her), “Simple Graphs' 8 Double-Irreducibility Classes", Online Encyclopaedia of Applied Graph and Order Theory, institute-theory-stem.org/oeagot-graph-double-irreducibility-classes/ (2026).

[50] E. Anderson, “The Fano Configuration, Plane and Graph", Online Encyclopaedia of Applied Graph and Order Theory, institute-theory-stem.org/fano/ (2026).

[51] “The Pappus Configuration, Theorem and Graph" Online Encyclopaedia of Applied Graph and Order Theory, institute-theory-stem.org/oeagot-pappus-graph/ (forthcoming 2026).

[52] “The Pappus Incidence Graph", Online Encyclopaedia of Applied Graph and Order Theory, institute-theory-stem.org/pappus-incidence-graph/ (2026).

[53] “The Smallest Cubic Graphs and their Cubeomorph Poset Arena" Online Encyclopaedia of Applied Graph and Order Theory, institute-theory-stem.org/oeagot-graphs-smallest-cubic-arenas/ (2026).

[54] Wikipedia, *Heawood Graph*, en.wikipedia.org/wiki/Pappus_graph , April 2026 version.

[55] E.W. Weisstein, “Heawood Graph." From MathWorld–A Wolfram Resource, mathworld.wolfram.com/PappusGraph.html , April 2026 version.

[56] The On-Line Encyclopedia of Integer Sequences, “Number of Unlabeled Trivalent (or Cubic) Connected Simple Graphs with $2n$ Nodes", https://oeis.org/A002851 .

[57] E. Anderson, “The Desargues Configuration, Theorem and Graph", Online Encyclopaedia of Applied Graph and Order Theory, institute-theory-stem.org/oeagot-desargues-graph/ (forthcoming 2026).

[58] “The Desargues Incidence Graph", Online Encyclopaedia of Applied Graph and Order Theory, institute-theory-stem.org/oeagot-desargues-incidence-graph/ (forthcoming 2026).

[59] A. Ford, “The Trees of Cubic Cage Theory", for [48] (forthcoming 2027).

[60] E. Anderson, “The Petersen Graph as a Counterexample to almost Everything" Online Encyclopaedia of Applied Graph and Order Theory, institute-theory-stem.org/oeagot-graphs-petersen/ (forthcoming 2027).

The above are Graph Theory references

Projective Geometry references

[61] L. Cremona, (1877), "Teoremi Stereometrici dal quali si deducono le proprietà dell' Esagrammo di Pascal", ("Stereometric Theorems from which the properties of Pascal's Hexagram are deduced") Atti R. Accademia Lincei **1** (1877).

[62] V. Martinetti, "Sopra alcune Configurazioni Piane", Ann. Mat. Pura ed Appl **14** 161 (1886).

[63] G. Fano, "Sui Postulati Fondamentali della Geometria Projettiva", (On the Fundamental Postulates of Projective Geometry) Gior. Mat. **30** 106 (1892).

[64] O. Veblen and J.W. Young, *Projective Geometry* (Ginn, Boston 1910).

[65] M. Hall Jr. (1943), "Projective Planes" Transact. Amer. Math. Soc. **54** 229 (1943).

[66] R.H. Bruck and H.J. Ryser, "The Nonexistence of certain Finite Projective Planes", Can. J. Math, **1** 88 (1949).

[67] J. Tits "Sur la Trialité et certains Groupes qui s'en Déduisent" ("On Triality and Certain Groups that derive from it"), Inst. Hautes ''Etudes Sci. Publ. Math. **2** 13 (1959).

[68] A. Seidenberg, *Lectures in Projective Geometry* (Van Nostrand, Princeton N.J. 1961; 2012).

[69] D. Pedoe, *An Introduction to Projective Geometry* (Pergamon, Oxford 1963).

[70] W. Feit and G. Higman, "The Non-existence of certain Generalized Polygons", J. Algebra **1** 114 (1964).

[71] H.S.M. Coxeter, *Projective Geometry* (Blaisdell 1964; 2003).

[72] A.F. Horadam, *A Guide to Undergraduate Projective Geometry* (Pergamon Press , Australia 1970).

[73] D. Hughes and F. Piper, *Projective Planes* (Springer-Verlag, 1973).

[74] S.E. Payne, "Finite Generalized Quadrangles: a survey", In Proc. Intern. Conf. Proj. Planes, p. 219 (Washington State U., 1973).

[75] S.E. Payne and J.A. Thas, "Finite Generalized Quadrangles". Research Notes in Mathematics, **110**. (Pitman, Boston, MA, 1984).

Title reissued by (E.M.S. 2009).

[76] D. Hughes and F. Piper, *Design Theory* (CUP, Cambridge 1985).

[77] *Handbook of Incidence Geometry*, ed. F. Buekenhout (Elsevier 1995).

[78] F. Buekenhout, "An Introduction to Incidence Geometry";

"Foundations of incidence Geometry", both in [77].

[79] J.A. Thas, "Generalized Polygons", in Handbook of Incidence Geometry ed. F. Buekenhout (Elsevier 1995).

[80] M. Boben, B. Grünbaum, T. Pisanski and A. Zitnik, "Small Triangle-free Configurations of Points and Lines", Discrete Comput. Geom. **35** 405 (2006).

[81] G.E. Moorhouse, "Incidence Geometry",

https://web.archive.org/web/20131029221809/http://www.uwyo.edu/moorhouse/handouts/incidence_geometry.pdf

(2007).

[82] C. Weibel, "Survey of Non-Desarguian Planes" Not. AMS **54** 1294 (2007).

[83] B. Grünbaum, *Configurations of Points and Lines* (A.M.S., Providence RI. 2009).

[84] J. Richter-Gebert, *Perspectives on Projective Geometry: A guide through Real and Complex Geometry* (Springer 2011).

[85] T. Pisanski and Brigitte Servatius, *Configurations from a Graphical Viewpoint*, (Birkhäuser, Boston 2013).

[86] M. Boben, B. Grünbaum and T. Pisanski, "Multilaterals in Configurations". Contrib. Alg. Geom **54** 263 (2013).

[87] A. Muller, M. Saniga, A. Giorgetti, H. de Boutray and F. Holweck, "Multi-qubit Doilies: Enumeration for all Ranks and Classification for Ranks Four and Five", J. Comput. Sci. **64**, October 101853 (2022), arXiv:2206.03599.

[88] G.E. Moorhouse, Projective Planes of Small Order https://ericmoorhouse.org/pub/planes/ (2026)

Other Geometry references

[89] B. Polster, *A Geometrical Picture Book* (Springer, New York 1998).

[90] J. Stillwell, *The Four Pillars of Geometry* (Springer, New York 2005).

[91] *Handbook of Combinatorial Designs* (2nd ed.) ed. C.J. Colbourn and J.H. Dinitz, (Chapman and Hall, Boca Raton FL. 2007).

[92] L. Storme, "Finite Geometry", in Design-Hand. In particular, pp. 719-727 review non-Desarguian planes at a level comparable to [82].

[93] C. Kimberling, *Encyclopedia of Triangle Centers*, https://faculty.evansville.edu/ck6/encyclopedia/ETC.html

[94] E. Anderson, *The Structure of Flat Geometry*, forthcoming (2026).

Order Theory references

[95] G. Birkhoff, *Lattice Theory* (A.M.S., Providence R.I., 1967).

[96] J. Neggers and H.S. Kim, *Basic Posets* (World Scientific, 1998).

[97] G. Grätzer, *General Lattice Theory* 2nd ed. (Birkhäuser Verlag, Basel 1998).

[98] B.A. Davey and Hilary A. Priestley, *Introduction to Lattices and Order* (C.U.P, Cambridge 2002).

[99] G. Grätzer *Lattice Theory: First Concepts and Distributive Lattices* (Courier 2009).

[100] *Lattice Theory: Foundation* (Springer Basel 2010).